Bifurcation analysis of pattern formation in a two-dimensional hybrid reaction-transport model

Sam R. Carroll[1], Heather Z. Brooks[2], Paul C. Bressloff[1]

[1] *Department of Mathematics, University of Utah, Salt Lake City, UT 84112 USA*

[2] *Department of Mathematics, UCLA, Los Angeles, CA 90095 USA*

Abstract

Following up on our work on Turing pattern formation in a one-dimensional reaction-transport model, we explore the emergence of patterns in a two dimensional model described by a system of PDEs for passively transported diffusing particles (PT) and actively transported motor-driven particles (AT). We first propose a model where the actively transported particles are taken to be functions of spatial locations $\mathbf{x} \in \mathbb{R}$ and velocity $\mathbf{v}$. We then consider two special simplifying cases where particles are transported at (i) constant speeds v so that the concentration of AT particles is taken to be a function of spatial location and velocity angle $\theta \in \mathbf{S}^1$ and (ii) discrete velocities (still with constant speed) in directions along a lattice tiling the plane. In the former case the system is equivariant with respect to the so called *shift-twist* action of the Euclidean group $\mathbf{E}(2)$ acting on functions on $\mathbb{R}^2 \times \mathbf{S}^1$, while in the latter case it is equivariant with respect to the group $\mathbf{D}_N \ltimes \mathbb{R}^2$ where $\mathbf{D}_N$ ($N = 4$ for square and $N = 6$ for hexagonal) is the holohedry group of the lattice. In both cases, we use symmetric bifurcation theory to analyze the planforms emerging from a Turing bifurcation, should it occur. In the discrete velocity square lattice case, we are able to prove that a Turing bifurcation does indeed occur as the dimensionless parameter $\gamma = \alpha D/v^2$ crosses some critical value. Here, D is the diffusion coefficient for the passively diffusing particles and α is the switching rate between motor states.

Keywords: motor-driven transport, switching dynamical systems, diffusion

1. Introduction

Recently, we proposed a novel mechanism for Turing pattern formation that provides a possible explanation for the formation and homeostatic control of regularly spaced synaptic puncta along the ventral cord of *C. elegans* during

Email addresses: carroll@math.utah.edu (Sam R. Carroll[1]), hbrooks@math.ucla.edu (Heather Z. Brooks[2]), bresslof@math.utah.edu (Paul C. Bressloff[1])

development [9]. The corresponding model consisted of two interacting chemical species, where one is passively diffusing and the other is actively trafficked by molecular motors. We identified the former as the protein kinase CaMKII and the latter as the glutamate receptor GLR-1. Motivated by the particular application to *C. elegans*, we considered a one-dimensional (1D) hybrid reaction-transport model, in which the motor-driven chemical switches between forward and backward moving states. Using linear stability analysis, we derived conditions on the associated nonlinear reaction functions for which a Turing instability can occur. In particular, we showed that the dimensionless quantity $\gamma = \alpha D/v^2$ had to be sufficiently small for patterns to emerge, where α is the switching rate between motor states, v is the motor speed, and D is the diffusion coefficient of CaMKII. We thus established that patterns cannot occur in the fast switching regime ($\alpha \to \infty$), which is the parameter regime where the model effectively reduces to a two-component reaction-diffusion system. Numerical simulations of the model using experimentally-based parameters generated patterns with a wavelength consistent with the synaptic spacing found in *C. elegans*, after identifying the in-phase CaMKII/GLR-1 concentration peaks as sites of new synapses. Extending the model to the case of a slowly growing 1D domain, we subsequently showed how the synaptic density can be maintained during *C. elegans* growth, due to the insertion of new concentration peaks as the length of the domain increases [10].

In this paper, we further explore the emergence of patterns in hybrid reaction-transport equations by considering a two-dimensional (2D) model. In the case of neurites of neurons in *C. elegans*, the microtubles tend to be aligned in parallel so that one can treat the active transport process as effectively 1D. On the other hand, intracellular transport within most non–polarized animal cells occurs along a microtubular network that projects radially from an organizing center (centrosome) with outward polarity [8]. This allows the transport of molecules to and from the nucleus, including viruses that take advantage of microtubule-based transport in order to reach the nucleus from the cell surface and release their genome [11]. A detailed microscopic model of intracellular transport within the cell would need to specify the spatial distribution of microtubular orientations and polarity, in order to specify which velocity states are available to a motor-cargo complex at a particular spatial location. However, a simplified model can be obtained under the "homogenization" assumption that the network is sufficiently dense so that the set of velocity states (and associated state transitions) available to the diffusing motor complex is independent of position. In that case, one can effectively represent active transport within the cell in terms of a higher-dimensional velocity jump process [1, 20, 6], which is analogous to an animal movement model with a turning function [17]. This provides a biological motivation for extending our previous model to higher dimensions. (For simplicity, we focus on a 2D model, which is a reasonable approximation for epithelial cells, for example.)

We consider two types of turning function: (i) all velocity directions are accessible to a particle independent of position (isotropic velocity case), and (ii) a finite set of velocity directions are accessible to a particle independent of

position, which are generated by a planar lattice (discrete velocity case). In both cases we derive conditions for the existence of a Turing bifurcation from a uniform state, and use the equivariant branching lemma [14, 25, 13, 18] to identify the planforms that emerge as primary bifurcations. In particular, we show that the planforms are nontrivial with regards the relative distribution of the active and passive chemical species. We note that the isotropic velocity version is a novel example of a PDE with so-called Euclidean shift-twist symmetry; the latter symmetry was originally identified within the context of a neural field model of visual hallucinations [3, 4]. However, as with previous applications, in order to exploit finite-dimensional bifurcation theory, it is necessary to restrict solutions to be doubly-periodic with respect to some planar lattice. One of the interesting features of the discrete velocity version is that the underlying microtubular network can provide a physical substrate for such a planar lattice.

The paper is organized as follows. The basic 1D hybrid reaction-transport model is presented in section 2. A 2D version of the model is introduced in section 3, where various microtubule network configurations are discussed. The possible symmetries of the 2D model are described in section 4, and these are then incorporated into the bifurcation analysis of 2D Turing patterns in sections 5 and 6. Note that in this paper we focus on the existence of Turing patterns and their symmetries. We do not determine their stability using, for example, weakly nonlinear analysis to derive a set of amplitude equations. In addition to the complexity of such an analysis, the resulting amplitude equations are not sufficient unless one has information about the explicit form of the nonlinearities and the corresponding model parameters. These are currently not known.

2. One-dimensional model

We begin by describing the 1D hybrid reaction-transport model of Ref. [9], which couples particles undergoing active bidirectional transport with a passively diffusing particle, see Fig. 1. Let $\mathcal{A}(x,t)$ denote the concentration of actively transported (AT) particles at position x at time t and let $P(x,t)$ denote the corresponding concentration of passively transported (PT) particles with diffusion coefficient D. We assume that each particle randomly switches between the two constant velocity states $\pm v_{\pm}$ according to a two-state Markov process with switching rate α. The AT particles are partitioned into two subpopulations: those that undergo anterograde (rightward) transport with positive velocity v_+ and density $A_+(x,t)$, and those that undergo retrograde (leftward) transport with negative velocity $-v_-$ and density $A_-(x,t)$:

$$\mathcal{A}(x,t) = A_+(x,t) + A_-(x,t). \tag{2.1}$$

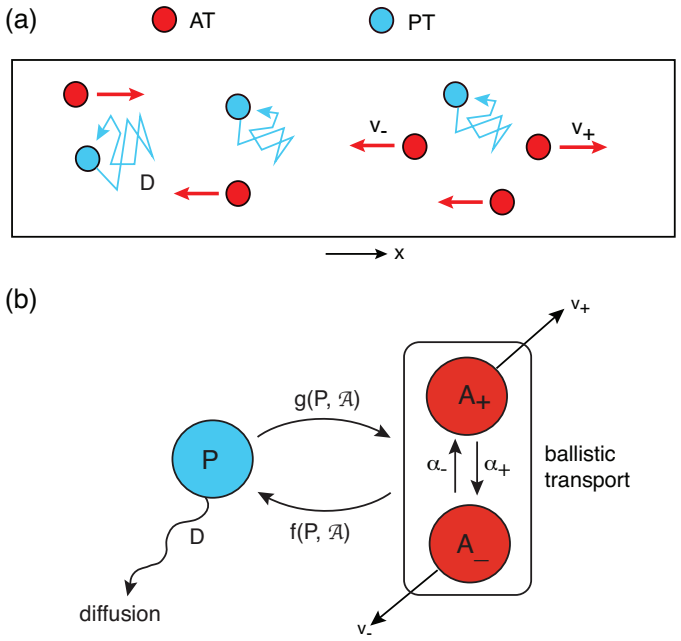

Figure 1: One-dimensional, three-component hybrid trafficking model. (a) Passively transported diffusing particles (PT) react with actively transported particles (AT). The latter switch between forward and backward moving states (traveling with velocities $\pm v_\pm$). (b) Reaction scheme of model.

The three-component system evolves according to the equations

$$\frac{\partial P}{\partial t} = D\frac{\partial^2 P}{\partial x^2} + f(P,\mathcal{A}) \tag{2.2a}$$

$$\frac{\partial A_+}{\partial t} = -v_+\frac{\partial A_+}{\partial x} - \alpha(A_+ - A_-) + g(P,\mathcal{A}) \tag{2.2b}$$

$$\frac{\partial A_-}{\partial t} = v_-\frac{\partial A_-}{\partial x} + \alpha(A_+ - A_-) + g(P,\mathcal{A}). \tag{2.2c}$$

The first term on the right-hand side of equation (2.2a) represents diffusive transport of PT particles and the first term on the right-hand side of equations (2.2b,c) represents ballistic transport of the AT particles to the right or left, respectively. The terms $\pm\alpha(A_+ - A_-)$ represent the effects of switching between the two advective states, which for simplicity are taken to be the same. The reaction terms f and g are taken to be functions of the PT particle concentration P and the total AT particle concentration $\mathcal{A}$.

It is important to note that three-component models analogous to (2.2) have been studied extensively within the context of population models of animal

movement and chemotaxis [21, 16, 17]. Chemotaxis refers to the active directed movement of cells along a chemical concentration gradient that is generated by the cells themselves, resulting in macroscopic cell aggregations. The chemical signal can affect both the rate of switching between different velocity rates and the velocities themselves. In the case of a 1D velocity-jump process, a chemotactic model takes the form

$$\frac{\partial P}{\partial t} = D\frac{\partial^2 P}{\partial x^2} + \kappa\mathcal{A} - \gamma P \tag{2.3a}$$

$$\frac{\partial A_+}{\partial t} = -\frac{\partial v(P)A_+}{\partial x} - \alpha^+(P,P_x)A_+ + \alpha^-(P,P_x)A_- \tag{2.3b}$$

$$\frac{\partial A_-}{\partial t} = \frac{\partial v(P)A_-}{\partial x} + \alpha^+(P,P_x)A_+ - \alpha^-(P,P_x)A_-. \tag{2.3c}$$

Here $P(x,t)$ represents the concentration of the diffusing chemotactic signal, which decays at a constant rate γ and is produced at a rate that is proportional to the total cell density $\mathcal{A} = A_+ + A_-$. The cells have concentration-dependent velocities $\pm v(P)$ and switching rates $\alpha^{\pm}(P,P_x)$. Note that the switching rates from the $+/-$ states are taken to be different. If we write $\alpha^{\pm}(P,P_x) = \alpha \mp \Phi(P)P_x$, then comparison with equations (2.2) shows that $v_\pm \to \pm v(P)$, $f(P,\mathcal{A}) \to \kappa\mathcal{A} - \gamma P$ and $g(P,\mathcal{A}) \to \pm\Phi(P)P_x\mathcal{A}$.

We recently used hybrid reaction-transport equations of the form (2.2) to analyze Turing patterns in a model for the formation of regularly spaced synaptic puncta along the ventral cord of *C. elegans* during development [9]. In this model we identified the PT particles as calcium-calmodulin protein kinase II (CaMKII) and the AT particles as glutamate receptors GLR-1 undergoing molecular motor-driven transport along microtubules (intracellular filaments). Using linear stability analysis we derived conditions on the associated nonlinear interaction functions f, g for which a Turing instability can occur. In the symmetric case ($v_\pm = v$) we found that the dimensionless quantity $\gamma = \alpha D/v^2$ had to be sufficiently small for patterns to emerge. One consequence is that patterns arise outside the parameter regime of fast switching, where the model effectively reduces to a classical two-component reaction-diffusion (RD) system. The absence of patterns in the RD model reflects the the fact that the AT particles are taken to be inhibitors and the PT particles to be activators, which holds for the particular application to synaptogenesis in *C. elegans* [9]. However, the diffusivity of the AT particles (inhibitors) is $O(\epsilon)$ in the fast switching limit. Note that in the particular application to *C. elegans*, we considered the classical activator-inhibitor system of Gierer and Meinhardt (GM) [12]:

$$f(P,\mathcal{A}) = \rho_1\frac{P^2}{\mathcal{A}} - \mu_1 P + \eta \tag{2.4a}$$

$$g(P,\mathcal{A}) = \rho_2 P^2 - \mu_2\mathcal{A}. \tag{2.4b}$$

Here ρ_1, ρ_2 represent the strength of interactions, μ_1 and μ_2 are the respective decay rates, and η is the production rate of CaMKII. The model was chosen as CaMKII exhibits autocatalysis, and we required the peaks of CaMKII and GLR-1 to be in-phase.

In our previous work we proved that a homogeneous fixed point to Equation (2.2) undergoes a Turing instability if the following inequalities hold [9]:

$$\gamma \equiv \frac{\alpha D}{v^2} < -\frac{f_P}{4g_A} < \frac{1}{2}, \quad g_A < 0, \quad f_P > 0, \quad f_A g_P < 0. \tag{2.5}$$

At the critical point, the fixed point is marginally stable with respect to excitation of a spatially periodic pattern of critical wavelength $2\pi/k_c$. Typically, varying one of the parameters of the underlying model can then push the associated real dispersion curve $\lambda = \lambda(k)$ above zero in a neighborhood of k_c, resulting in a Turing instability. Whether or not a stable periodic pattern forms then depends on the nonlinearities of the system, which can be investigated numerically or using weakly nonlinear analysis.

3. Two-dimensional model

We now consider a 2D hybrid reaction-transport model. Let $P(\mathbf{x}, t)$ denote the concentration of PT particles at position $\mathbf{x} \in \mathbb{R}^2$ at time t. Similarly, let $A(\mathbf{x}, \mathbf{v}, t)$ denote the corresponding concentration of AT particles with velocity $\mathbf{v} \in V \subset \mathbb{R}^2$. The 2D generalization of equations (2.2) takes the form

$$\frac{\partial P}{\partial t} = D\nabla^2 P + f(P, \mathcal{A}) \tag{3.1a}$$

$$\frac{\partial A}{\partial t} = -\mathbf{v} \cdot \nabla A - \alpha A + \alpha \int_V T(\mathbf{v}, \mathbf{v}') A(\mathbf{x}, \mathbf{v}', t) d\mathbf{v}' + g(P, \mathcal{A}), \tag{3.1b}$$

where

$$\mathcal{A}(\mathbf{x}, t) = \int_V A(\mathbf{x}, \mathbf{v}, t) d\mathbf{v}, \tag{3.2}$$

and $T(\mathbf{v}, \mathbf{v}')$ is the so-called turning distribution [15]. The latter describes the probability that an AT particle with velocity $\mathbf{v}'$ switches to the velocity $\mathbf{v}$. Analytical properties of the associated turning operator and various biology constraints have been discussed in detail elsewhere [15, 21, 17], particularly within the context of animal movement models. Here we consider turning functions relevant to intracellular transport [7]. In particular, we assume that T is invariant under the change $(\mathbf{v}, \mathbf{v}') \mapsto (\sigma\mathbf{v}, \sigma\mathbf{v}')$ for $\sigma \in \mathbf{O}(2)$ since this transformation leaves distance and angle between $\mathbf{v}$ and $\mathbf{v}'$ unchanged. In the following section we will describe the symmetries of the full model under this constraint, and then discuss some special cases.

3.1. Symmetries of the full model

It is well known that standard reaction-diffusion equations in $\mathbb{R}^2$ are equivariant with respect to the action of the Euclidean group $\mathbf{E}(2)$, which is composed of the semi-direct product of the group of planar rotations and reflections ($\mathbf{O}(2)$) and the group of planar translations ($\mathbb{R}^2$). That is, define the *action* of the group $\mathbf{E}(2)$ on functions $u(\mathbf{x})$ as

$$\sigma \cdot u(\mathbf{x}) = u(\sigma^{-1}\mathbf{x}), \quad \forall \sigma \in \mathbf{E}(2),$$

where $\sigma^{-1}\mathbf{x}$ is the inverse of the usual rotation, reflection and translation of vectors $\mathbf{x} \in \mathbb{R}^2$. The system

$$\frac{\partial u}{\partial t} = G(u),$$

where G maps the space of functions into itself, is said to be *equivariant* with respect to the action of $\mathbf{E}(2)$ if $\sigma \cdot G(u) = G(\sigma \cdot u)$ for all $\sigma \in \mathbf{E}(2)$ and all functions u. For example, suppose that there are only PT particles so that equation (3.1a) becomes

$$\frac{\partial P(\mathbf{x}, t)}{\partial t} = D\nabla^2 P + f(P).$$

It is straightforward to show that ∇^2 is $\mathbf{E}(2)$ equivariant and that f is simply a function of the argument (thus trivially equivariant), so the full system is $\mathbf{E}(2)$ equivariant.

One major consequence of equivariant systems is that if $u(\mathbf{x}, t)$ is a solution, then so is $u(\sigma^{-1}\mathbf{x}, t)$ for any $\sigma \in \mathbf{E}(2)$. Moreover, the linearization of the system about some homogeneous stationary solution $u(\mathbf{x}) \equiv u_0$ is also equivariant. That is, if we write

$$\frac{\partial u}{\partial t} = \mathbb{L}u$$

with $\mathbb{L} = DG|_{u_0}$ (the differential of G at u_0) and $u(\mathbf{x})$ is an eigenfunction of $\mathbb{L}$ then so are $u(\sigma^{-1}\mathbf{x})$, and the associated eigenvalues are the same. Whenever the group contains translations, as it does with $\mathbf{E}(2)$, then generically, eigenfunctions of $\mathbb{L}$ are of the form $e^{i\mathbf{k}\cdot\mathbf{x}}$ with the eigenvalues depending on the wavevector $\mathbf{k}$. Additionally, if the group contains rotations, then we have a one-parameter family of eigenfunctions $e^{i\mathbf{k}\cdot(R_{-\phi}\mathbf{x})} = e^{i(R_\phi\mathbf{k})\cdot\mathbf{x}}$ ($\phi \in [0, 2\pi)$). In this case, the eigenvalues only depend on the magnitude of $\mathbf{k}$, i.e. $\lambda = \lambda(||\mathbf{k}||)$. It follows that for a system of reaction-diffusion equations exhibiting a Turing bifurcation (from a uniform steady state to a globally patterned state with a dominant finite wavenumber k_c), there are an infinite number of marginally stable modes lying on the critical circle $||\mathbf{k}|| = k_c$. The standard way of handling this infinite degeneracy is to require that solutions are doubly-periodic with respect to one of the planar lattices listed in Table 3.1 below, resulting in a finite-dimensional bifurcation problem [25, 13, 18].

Let us now turn our attention back to the hybrid reaction-transport system (3.1). This system is not equivariant with respect to the standard action of $\mathbf{E}(2)$. First of all, the function A not only depends on $\mathbf{x}$ but also on the velocity $\mathbf{v}$. Hence we must define the action on variables $(\mathbf{x}, \mathbf{v}) \in \mathbb{R}^2 \times V$. Second, the kernel $T(\mathbf{v}, \mathbf{v}')$ of the integral operator must have a particular structure. Imposing the $\mathbf{O}(2)$ symmetry of T, we define the Euclidean action on functions $(P(\mathbf{x}), A(\mathbf{x}, \mathbf{v}))$ as follows:

$$\sigma \cdot (P(\mathbf{x}), A(\mathbf{x}, \mathbf{v})) = \begin{cases} (P(\sigma^{-1}\mathbf{x}), A(\sigma^{-1}\mathbf{x}, \sigma^{-1}\mathbf{v})), & \sigma \in \mathbf{O}(2) \\ (P(\sigma^{-1}\mathbf{x}), A(\sigma^{-1}\mathbf{x}, \mathbf{v})), & \sigma \in \mathbb{R}^2. \end{cases} \tag{3.3}$$

By changing variables $\mathbf{v}' \to \sigma\mathbf{v}'$, and noting that $\sigma V = V$ and $d(\sigma\mathbf{v}') = d\mathbf{v}'$, we have

$$\int_V A(\sigma^{-1}\mathbf{x}, \sigma^{-1}\mathbf{v}')d\mathbf{v}' = \int_V A(\sigma^{-1}\mathbf{x}, \mathbf{v}')d\mathbf{v}', \quad \forall\sigma \in \mathbf{O}(2),$$

which shows that $\int A$ is $\mathbf{E}(2)$-equivariant. Since f and g are functions of P and $\int A$, it follows that the f and g terms are $\mathbf{E}(2)$-equivariant. Moreover, since $\mathbf{E}(2)$ acts on P in the standard way, it follows that ∇^2 is $\mathbf{E}(2)$-equivariant. Thus it remains to show that the gradient and integral operator are equivariant.

First, we consider the integral operator. For $\sigma \in \mathbf{O}(2)$, we must show

$$\sigma \cdot \int_V T(\mathbf{v}, \mathbf{v}')A(\mathbf{x}, \mathbf{v}', t)d\mathbf{v}' = \int_V T(\mathbf{v}, \mathbf{v}')[\sigma \cdot A(\mathbf{x}, \mathbf{v}', t)]d\mathbf{v}'.$$

We have

$$\begin{aligned}
\sigma \cdot \int_V T(\mathbf{v}, \mathbf{v}')A(\mathbf{x}, \mathbf{v}', t)d\mathbf{v}' &= \int_V T(\sigma^{-1}\mathbf{v}, \mathbf{v}')A(\sigma^{-1}\mathbf{x}, \mathbf{v}', t)d\mathbf{v}' \\
&= \int_V T(\sigma^{-1}\mathbf{v}, \sigma^{-1}\mathbf{v}')A(\sigma^{-1}\mathbf{x}, \sigma^{-1}\mathbf{v}', t)d\mathbf{v}' \\
&= \int_V T(\mathbf{v}, \mathbf{v}')A(\sigma^{-1}\mathbf{x}, \sigma^{-1}\mathbf{v}', t)d\mathbf{v}' \\
&= \int_V T(\mathbf{v}, \mathbf{v}')[\sigma \cdot A(\mathbf{x}, \mathbf{v}', t)]d\mathbf{v}'
\end{aligned}$$

where the second line comes from the change of variables $\mathbf{v}' \to \sigma^{-1}\mathbf{v}'$, and the third line comes from the $\mathbf{O}(2)$ invariance assumption for T. Now consider the gradient term. We must show that

$$[\sigma^{-1}\mathbf{v}] \cdot [\nabla_{\mathbf{x}} A(\mathbf{x}, \mathbf{v})]\big|_{(\mathbf{x},\mathbf{v})\to(\sigma^{-1}\mathbf{x},\sigma^{-1}\mathbf{v})} = \mathbf{v} \cdot \nabla_{\mathbf{x}}[A(\sigma^{-1}\mathbf{x}, \sigma^{-1}\mathbf{v}))].$$

Standard multivariate calculus shows that

$$\nabla f(\sigma^{-1}\mathbf{x}) = [\sigma\nabla f(\mathbf{x})]\big|_{\mathbf{x}\to\sigma^{-1}\mathbf{x}}, \quad \forall\sigma \in \mathbf{O}(2)$$

and therefore

$$\begin{aligned}
\mathbf{v} \cdot \nabla_{\mathbf{x}}[A(\sigma^{-1}\mathbf{x}, \sigma^{-1}\mathbf{v})] &= \mathbf{v} \cdot [\sigma\nabla_{\mathbf{x}} A(\mathbf{x}, \mathbf{v})]\big|_{(\mathbf{x},\mathbf{v})\to(\sigma^{-1}\mathbf{x},\sigma^{-1}\mathbf{v})} \\
&= \left[\sigma^T\mathbf{v}\right] \cdot [\nabla_{\mathbf{x}} A(\mathbf{x}, \mathbf{v})]\big|_{(\mathbf{x},\mathbf{v})\to(\sigma^{-1}\mathbf{x},\sigma^{-1}\mathbf{v})} \\
&= \left[\sigma^{-1}\mathbf{v}\right] \cdot [\nabla_{\mathbf{x}} A(\mathbf{x}, \mathbf{v})]\big|_{(\mathbf{x},\mathbf{v})\to(\sigma^{-1}\mathbf{x},\sigma^{-1}\mathbf{v})}.
\end{aligned}$$

Note that the second line follows from the definition of the adjoint with respect to the standard dot product, and the third line follows from the orthogonality of $\sigma \in \mathbf{O}(2)$. Furthermore, it is clear that the integral operator is equivariant with respect to translations $(\mathbf{x}, \mathbf{v}) \to (\mathbf{x} + \mathbf{a}, \mathbf{v})$. Hence, equation (3.1) is $\mathbf{E}(2)$ equivariant.

If the nonlinearities f and g are odd functions of their arguments then the system has additional symmetry. In this case, define the *pseudoscalar action* by

$$\sigma^p \begin{bmatrix} P \\ A \end{bmatrix} = \begin{cases} \sigma^s \begin{bmatrix} P \\ A \end{bmatrix}, & \text{if } \sigma^s \text{ is a rotation or translation} \\ -\sigma^s \begin{bmatrix} P \\ A \end{bmatrix}, & \text{if } \sigma^s \text{ is a reflection} \end{cases} \tag{3.4}$$

where σ^s is the *scalar* action defined in equation (3.3). Then equation (3.1) is equivariant with respect to this action if and only if f and g are odd functions. Linear systems do not distinguish between scalar and pseudoscalar actions, since all linear operators equivariant with respect to the scalar action are also equivariant with respect to the pseudoscalar action. Hence the same eigenfunctions will arise in both cases. The difference occurs at the nonlinear level when analyzing the selection of patterns through the Turing bifurcation.

3.2. Isotropic velocities and Euclidean shift-twist symmetry

Intracellular transport within most non–polarized animal cells occurs along a microtubular network projecting radially from an organizing centers or centrosomes [8]. Large internal stresses can often bend the microtubles, resulting in a locally disordered network, see Fig. 2. It follows that *in vivo* transport on relatively short length scales may be similar to transport observed *in vitro*, where microtubular networks are not grown from a centrosome and thus exhibit orientational and polarity disorder [23, 19]. In the case of a highly disordered, dense network one can make the simplifying assumption that all velocity directions are accessible to an AT particle independently of position. If we take the speed to be the same in all directions, then $\mathbf{v}$ can be parameterized by the direction angle $\theta \in [0, 2\pi)$

$$\mathbf{v}(\theta) = v(\cos\theta, \sin\theta).$$

Setting $A = A(\mathbf{x}, \theta, t)$ and $T(\mathbf{v}(\theta), \mathbf{v}(\theta')) = T(\theta - \theta')$ with $T(\theta)$ an even function, equations (3.1) become [6]

$$\frac{\partial P}{\partial t} = D\nabla^2 P + f(P, \mathcal{A}) \tag{3.5a}$$

$$\frac{\partial A}{\partial t} = -\mathbf{v}(\theta)\cdot\nabla A - \alpha A + \alpha \int_0^{2\pi} T(\theta - \theta') A(\mathbf{x}, \theta', t) d\theta' + g(P, \mathcal{A}), \tag{3.5b}$$

with

$$\mathcal{A}(\mathbf{x}, t) = \int_0^{2\pi} A(\mathbf{x}, \theta, t) d\theta. \tag{3.6}$$

Note that T has this particular form since $T(\mathbf{v}, \mathbf{v}')$ is $\mathbf{O}(2)$ invariant and thus depends on the difference in angles. In the subsequent analysis, it will be convenient to non-dimensionalize this system by performing the change of variables

$$\mathbf{x} \to \frac{v}{\alpha}\mathbf{x}, \quad t \to \frac{1}{\alpha}t, \quad f \to \frac{1}{\alpha}f, \quad g \to \frac{1}{\alpha}g$$

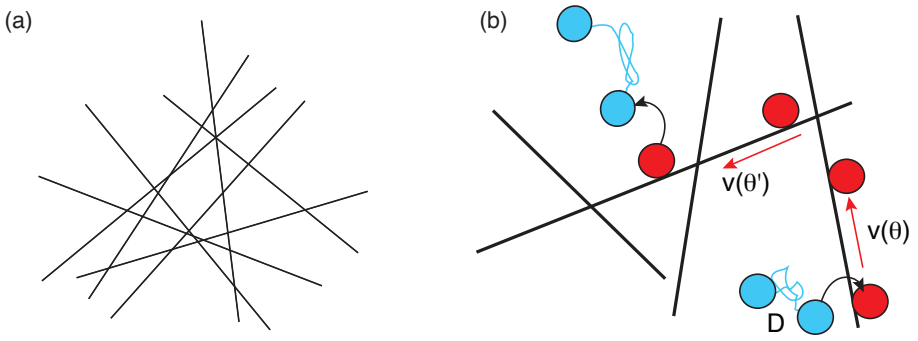

Figure 2: Disordered microtubular network. (a) Random orientational arrangement of microtubules. (b) Hybrid 2D transport in which a particle switches between diffusion and ballistic motion in a random direction θ. We ignore the polarization of each filament, since we assume that a bound particle can reverse its direction along a given filament, as in the 1D model.

to obtain the system

$$\frac{\partial P}{\partial t} = \gamma \nabla^2 P + f(P, \mathcal{A}) \tag{3.7a}$$

$$\frac{\partial A}{\partial t} = -\vec{\theta} \cdot \nabla A - A + \int_0^{2\pi} T(\theta - \theta') A(\mathbf{x}, \theta', t) d\theta' + g(P, \mathcal{A}), \tag{3.7b}$$

where we define $\gamma = \alpha D / v^2$ and $\vec{\theta} = (\cos\theta, \sin\theta)$. In the analysis below we will use γ as the bifurcation parameter.

The action defined in equation (3.3) induces a corresponding action of the Euclidean group on the product space $\mathbb{R}^2 \times \mathbf{S}^1$, where $\mathbf{S}^1$ denotes the circle. Rotations and reflections act on $\mathbf{S}^1$ according to

$$R_\phi \mathbf{v}(\theta) = R_\phi v(\cos\theta, \sin\theta) = v(\cos(\theta + \phi), \sin(\theta + \phi))$$

and

$$\kappa \mathbf{v}(\theta) = \kappa v(\cos\theta, \sin\theta) = v(\cos\theta, -\sin\theta) = v(\cos\theta, \sin(-\theta))$$

and therefore the corresponding action on $\mathbb{R}^2 \times \mathbf{S}^1$ is

$$\begin{array}{rcll} \mathbf{s} \cdot (\mathbf{x}, \theta) & = & (\mathbf{x} + \mathbf{s}, \theta) & \mathbf{s} \in \mathbb{R}^2 \\ \varphi \cdot (\mathbf{x}, \theta) & = & (R_\varphi \mathbf{x}, \theta + \varphi) & \varphi \in \mathbf{S}^1 \\ \kappa \cdot (\mathbf{x}, \theta) & = & (\kappa \mathbf{x}, -\theta). & \end{array} \tag{3.8}$$

We define the action on vector functions $(P(\mathbf{x}), A(\mathbf{x}, \theta))$ by

$$\sigma \cdot \begin{bmatrix} P(\mathbf{x}) \\ A(\mathbf{x}, \theta) \end{bmatrix} = \begin{bmatrix} P(\sigma^{-1}\mathbf{x}) \\ A(\sigma^{-1} \cdot (\mathbf{x}, \theta)) \end{bmatrix} \quad \text{for all } \sigma \in \mathbf{E}(2), \tag{3.9}$$

where $\sigma^{-1}\mathbf{x}$ means the standard Euclidean action on $\mathbb{R}^2$. The same so-called *shift-twist* Euclidean group action occurs within the context of continuum neural

Lattice	$\boldsymbol{\ell}_1$	$\boldsymbol{\ell}_2$	$\hat{\boldsymbol{\ell}}_1$	$\hat{\boldsymbol{\ell}}_2$
Square	$(1,0)$	$(0,1)$	$(1,0)$	$(0,1)$
Hexagonal	$(1,0)$	$\frac{1}{2}(-1,\sqrt{3})$	$(1,\frac{1}{\sqrt{3}})$	$(0,\frac{2}{\sqrt{3}})$
Rhombic	$(1,0)$	$(\cos\eta,\sin\eta)$	$(1,-\cot\eta)$	$(0,\csc\eta)$

Table 1: Generators for the planar lattices and their dual lattices in the case of unit lattice spacing ($d=1$). The generators of the dual lattice satisfy $\boldsymbol{\ell}_i \cdot \hat{\boldsymbol{\ell}}_j = \delta_{i,j}$.

field models of primary visual cortex, where non–local interactions are mediated by axonal connections between neurons that are tuned to respond to oriented visual stimuli [3, 4, 24]. They also arise in a general class of non–local population models describing the aggregation and alignment of oriented objects in two dimensions, including protein filaments and oriented cells such as fibroblasts [5].

The proof of equivariance of the hybrid reaction-transport equations (3.5) immediately follows from the proof in §3.1. Additionally, the system is equivariant with respect to the pseudoscalar action in equation (3.4) if and only if f and g are odd functions. Equivariance with respect to the shift-twist action of the Euclidean group means that the bifurcation analysis of marginally stable Turing patterns has to deal with the infinite degeneracy arising from rotation symmetry. In order to handle the infinite degeneracy of the dispersion curves, one can restrict the class of solutions to be doubly-periodic with respect to a regular planar lattice $\mathcal{L}$. The lattice $\mathcal{L}$ is generated by two linearly independent vectors $\boldsymbol{\ell}_1$ and $\boldsymbol{\ell}_2$:

$$\mathcal{L} = \{(m_1\boldsymbol{\ell}_1 + m_2\boldsymbol{\ell}_2) : \ m_1, m_2 \in \mathbb{Z}\} \tag{3.10}$$

with lattice spacing $d = |\boldsymbol{\ell}_j|$. Let ψ be the angle between the two basis vectors $\boldsymbol{\ell}_1$ and $\boldsymbol{\ell}_2$. We can then distinguish three types of lattice according to the value of ψ: square lattice ($\psi = \pi/2$), rhombic lattice ($0 < \psi < \pi/2$, $\psi \neq \pi/3$) and hexagonal ($\psi = \pi/3$), see Table 1 and Fig. 3. The three lattices have distinct holohedries, which are the subgroup of rotations and reflections $\mathbf{O}(2)$ that preserves the lattice. The holohedry of the rhombic lattice is $\mathbf{D}_2$, the holohedry of the square lattice is $\mathbf{D}_4$, and the holohedry of the hexagonal lattice is $\mathbf{D}_6$. This implies that there are only a finite number of rotations and reflections to consider for each lattice. A function $f : \mathbb{R}^2 \times \mathbf{S}^1 \to \mathbb{R}$ is *doubly periodic* with respect to $\mathcal{L}$ if

$$f(\mathbf{x} + \boldsymbol{\ell}, \theta) = f(\mathbf{x}, \theta)$$

for every $\boldsymbol{\ell} \in \mathcal{L}$. Restriction to double periodicity means that the original Euclidean symmetry group is now restricted to the symmetry group of the lattice, $\Gamma = \mathbf{D}_N \ltimes \mathbf{T}^2$

3.3. Discrete velocities and holohedral symmetry

We now consider an alternative microtubular network configuration, where the filaments form a dense mesh that tiles the plane, so that at any point $\mathbf{x}$, a

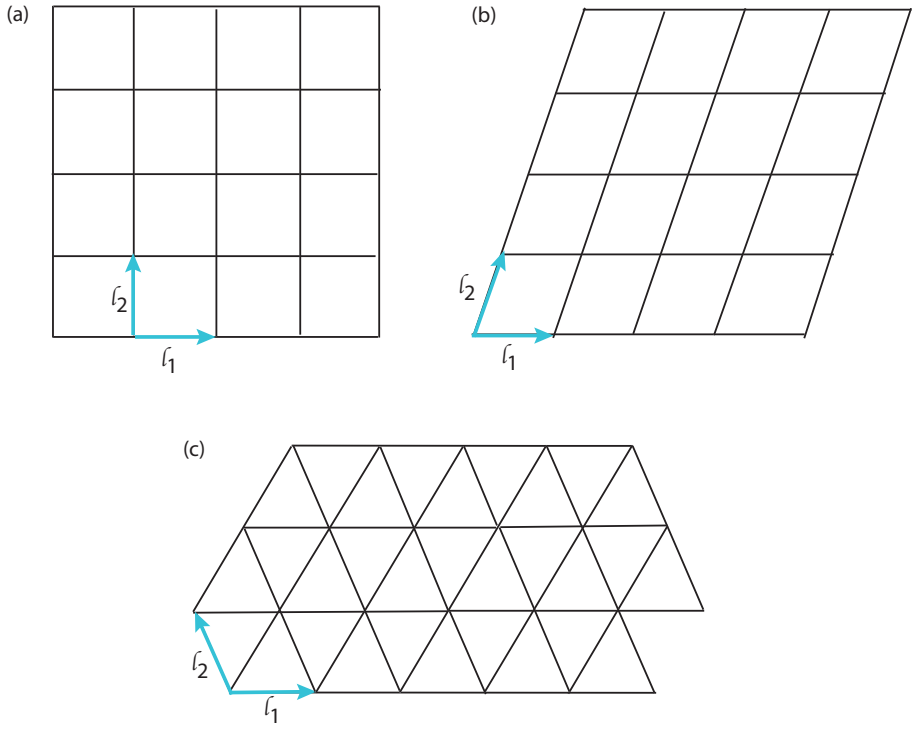

Figure 3: Regular planar lattices. (a) Square configuration ($\mathbf{D}_4$). (b) Rhombic configuration ($\mathbf{D}_2$). (c) Hexagonal configuration ($\mathbf{D}_6$).

particle switches between a discrete set of velocities. As a further simplification, suppose that the mesh is formed by one of the regular planar lattices $\mathcal{L}$ shown in Fig. 3. As in the case of the disordered network, we assume that the filaments are sufficiently dense and an AT particle can move with speed $\pm v$ in any of the discrete directions. In other words, the different ballistic states of an AT particle are given by

$$\mathbf{v} = \pm v\boldsymbol{\ell}_1, \quad \pm v\boldsymbol{\ell}_2$$

for the square and rhombic configurations, and

$$\mathbf{v} = \pm v\boldsymbol{\ell}_1, \quad \pm v\boldsymbol{\ell}_2, \quad \pm v(\boldsymbol{\ell}_1 + \boldsymbol{\ell}_2)$$

for the hexagonal configuration. It is important to observe that for a dense network, the lattice structure determines the set of velocity states available to an AT particle - it does not affect the dependence of concentrations on the spatial variable $\mathbf{x}$. This is distinct from the role that planar lattices play in the analysis of reaction-diffusion systems with Euclidean symmetry, where one imposes double-periodicity with respect to the lattice in order to deal with infinite degeneracies, see section 4.

Suppose that the different velocity states are labeled by $j = 0, \ldots, N-1$ with $N = 4$ (square, rhombic lattice) or $N = 6$ (hexagonal lattice). We assume that each velocity state is equally likely. After non-dimensionalizing as in §3.2, equation (3.1) becomes

$$\frac{\partial P}{\partial t} = \gamma \nabla^2 P + f(P, \mathcal{A}) \tag{3.11a}$$

$$\frac{\partial A_j}{\partial t} = -\boldsymbol{\ell}_j \cdot \nabla A_j - A_j + \frac{1}{N-1} \sum_{n=0, \neq j}^{N-1} A_n(\mathbf{x}, t) + g(P, \mathcal{A}), \tag{3.11b}$$

where

$$\mathcal{A}(\mathbf{x}, t) = \sum_{j=0}^{N-1} A_n(\mathbf{x}, t) \tag{3.12}$$

and A_j denotes the concentration of AT particles in velocity state $\mathbf{v}_j = v\boldsymbol{\ell}_j$, where $\boldsymbol{\ell}_j$ are the lattice vectors defined in Table (1). Note that the summation on the right-hand side of equation (3.11a) does not include A_j, since this represents transitions out of the state j. Each transition is equally likely, so that we have the normalization $1/(N-1)$.

The discrete velocity model explicitly breaks continuous $\mathbf{O}(2)$ symmetry. In particular, Equations (3.11) are equivariant with respect to the semi-direct product group $\Gamma = \mathbf{D}_N \ltimes \mathbb{R}^2$ acting on the space $\mathbb{R}^2 \times V$, where $\mathbf{D}_N$ is the associated lattice holohedry and V is the discrete set of velocities. The action on the square lattice is generated by

$$\begin{aligned}
\mathbf{s} \cdot (\mathbf{x}, \mathbf{v}_j) &= (\mathbf{x} + \mathbf{s}, \mathbf{v}_j) \quad \mathbf{s} \in \mathbb{R}^2 \\
R_{\pi/2} \cdot (\mathbf{x}, \mathbf{v}_j) &= (R_{\pi/2}\mathbf{x}, R_{\pi/2}\mathbf{v}_j) = (R_{\pi/2}\mathbf{x}, \mathbf{v}_{j+1}),\ j = 0, 1, 2, 3 \bmod 4 \\
\kappa \cdot (\mathbf{x}, \mathbf{v}_j) &= (\kappa\mathbf{x}, \kappa\mathbf{v}_j) = \begin{cases} (\kappa\mathbf{x}, \mathbf{v}_j), & j = 0, 2 \\ (\kappa\mathbf{x}, \mathbf{v}_{j+2}), & j = 1, 3 \bmod 4 \end{cases}
\end{aligned} \tag{3.13}$$

where κ is reflection across the first component (x-axis) and $\mathbf{v}_j = \mathbf{v}(j\pi/2)$. Similarly, the action on the hexagonal lattice is

$$\begin{aligned}
\mathbf{s} \cdot (\mathbf{x}, \mathbf{v}_j) &= (\mathbf{x} + \mathbf{s}, \mathbf{v}_j) \quad \mathbf{s} \in \mathbb{R}^2 \\
R_{\pi/3} \cdot (\mathbf{x}, \mathbf{v}_j) &= (R_{\pi/3}\mathbf{x}, R_{\pi/3}\mathbf{v}_j) = (R_{\pi/3}\mathbf{x}, \mathbf{v}_{j+1}),\ j = 0, 1, \ldots, 5 \bmod 6 \\
\kappa \cdot (\mathbf{x}, \mathbf{v}_j) &= (\kappa\mathbf{x}, \kappa\mathbf{v}) = \begin{cases} (\kappa\mathbf{x}, \mathbf{v}_j), & j = 0, 3 \\ (\kappa\mathbf{x}, \mathbf{v}_5), & j = 1 \\ (\kappa\mathbf{x}, \mathbf{v}_4), & j = 2 \end{cases}
\end{aligned} \tag{3.14}$$

where $\mathbf{v}_j = \mathbf{v}(j\pi/3)$. Note that the action on V can be equivalently expressed in terms of permutations of the index j, $j \to \sigma(j)$. The corresponding group action on the functions $A_j(\mathbf{x})$ is given by

$$\sigma \cdot A_j(\mathbf{x}) = A_{\sigma^{-1}(j)}(\sigma^{-1} \cdot \mathbf{x}) \quad \text{for all } \sigma \in \mathbf{D}_N. \tag{3.15}$$

Thus we define the action of Γ on functions $(P, \mathbf{A})^T$ as

$$\sigma \begin{bmatrix} P(\mathbf{x}) \\ \mathbf{A}(\mathbf{x}) \end{bmatrix} = \begin{cases} \begin{bmatrix} P(\sigma^{-1}\mathbf{x}) \\ \mathbb{P}_\sigma^{-1}\mathbf{A}(\sigma^{-1}\mathbf{x}) \end{bmatrix}, & \forall \sigma \in \mathbf{D}_N \\ \begin{bmatrix} P(\sigma^{-1}\mathbf{x}) \\ \mathbf{A}(\sigma^{-1}\mathbf{x}) \end{bmatrix}, & \forall \sigma \in \mathbb{R}^2 \end{cases} \tag{3.16}$$

where $\mathbf{A} = (A_0, ..., A_{N-1})^T$ and $\mathbb{P}_\sigma$ is the permutation matrix corresponding to σ. With this action, equation (3.11) is Γ-equivariant. Once again, the system is also equivariant with respect to the scalar action if and only if f and g are odd functions.

4. Properties of the linearized system

4.1. Isotropic velocities

For simplicity, we take a uniform turning distribution $T(\theta) = 1/2\pi$. Suppose there exists a homogeneous fixed point of equation (3.7) given by

$$(P(\mathbf{x}, t), A(\mathbf{x}, \theta, t)) = (P^*, A^*).$$

Linearizing about this fixed point yields the spectral problem

$$\lambda p(\mathbf{x}) = \gamma \nabla^2 p(\mathbf{x}) + f_P p(\mathbf{x}) + f_A \int a(\mathbf{x}, \theta) d\theta \tag{4.1a}$$

$$\lambda a(\mathbf{x}, \theta) = -\vec{\theta} \cdot \nabla a(\mathbf{x}, \theta) - a(\mathbf{x}, \theta) + \left(\frac{1}{2\pi} + g_A \right) \int a(\mathbf{x}, \theta) d\theta + g_P p(\mathbf{x}). \tag{4.1b}$$

These equations can be rewritten in the form

$$\lambda \begin{bmatrix} p \\ a \end{bmatrix} = \mathbb{L} \begin{bmatrix} p \\ a \end{bmatrix},$$

with the linear operator $\mathbb{L}$ acting on $C^2(\mathbb{R}^2 \times \mathbf{S}^1, \mathbb{R}^2)$. The fact that $\mathbb{L}$ commutes with the action of $\mathbf{O}(2) \ltimes \mathbb{R}^2$ greatly reduces the complexity of the spectral problem. First, translation symmetry implies that eigenfunctions are of the form

$$\begin{bmatrix} p(\mathbf{x}) \\ a(\mathbf{x}, \theta) \end{bmatrix} = \mathbf{w}(\mathbf{k}, \theta) \equiv \mathbf{u}(\theta) e^{i\mathbf{k}\cdot\mathbf{x}} + c.c, \quad \mathbf{u}(\theta) = \begin{bmatrix} p \\ a(\theta) \end{bmatrix} \tag{4.2}$$

where $\mathbf{k} \in \mathbb{R}^2$, $p \in \mathbb{C}$ and $a(\theta)$ is a complex valued 2π-periodic function. Substituting (4.2) into equations (4.1) yields the eigenvalue problem

$$\lambda(\mathbf{k}) p = (-\gamma ||\mathbf{k}||^2 + f_P) p + f_A \int_0^{2\pi} a(\theta) d\theta \tag{4.3a}$$

$$\lambda(\mathbf{k}) a(\theta) = -\left(i\vec{\theta} \cdot \mathbf{k} + 1 \right) a(\theta) + \left(\frac{1}{2\pi} + g_A \right) \int_0^{2\pi} a(\theta) d\theta + g_P p. \tag{4.3b}$$

The right-hand side defines the linear operator $\mathbb{L}$ acting on complex, vector-valued, 2π-periodic functions $\mathbf{u}(\theta)$ with parameter $\mathbf{k}$. Hence, we can treat the eigenvalues as functions of $\mathbf{k}$. Equivariance implies that $\lambda(\mathbf{k}) = \lambda(\sigma\mathbf{k})$ for all $\sigma \in \mathbf{O}(2)$, so that if $\mathbf{u}(\theta)$ is an eigenfunction of $\lambda(\mathbf{k})$ then $\mathbf{u}(\sigma^{-1}\theta)$ is an eigenfunction of $\lambda(\sigma\mathbf{k})$. This follows from

$$\sigma[\mathbf{u}(\theta)e^{\lambda t+i\mathbf{k}\cdot\mathbf{x}}] = \mathbf{u}(\sigma^{-1}\theta)e^{\lambda t+i\mathbf{k}\cdot(\sigma^{-1}\mathbf{x})} = \mathbf{u}(\sigma^{-1}\theta)e^{\lambda t+i(\sigma\mathbf{k})\cdot\mathbf{x}}$$

by properties of the standard dot product, and σ being represented by orthogonal matrices. It is clear that the eigenvalues of $\mathbb{L}$ only depend on the magnitude $||\mathbf{k}|| = k$ and thus, without loss of generality, we can take $\mathbf{k} = k(1,0)$ and study the reduced system

$$\lambda p = \quad (-\gamma k^2 + f_P)p + f_A \int_0^{2\pi} a(\theta)d\theta \tag{4.4a}$$

$$\lambda a(\theta) = \quad -(ik\cos(\theta)+1)\,a(\theta) + \left(\frac{1}{2\pi} + g_A\right)\int_0^{2\pi} a(\theta)d\theta + g_P p, \tag{4.4b}$$

which we rewrite in the more compact form

$$\lambda \begin{bmatrix} p \\ a(\theta) \end{bmatrix} = \mathbb{L}_0(k) \begin{bmatrix} p \\ a(\theta) \end{bmatrix}. \tag{4.5}$$

Then, given an eigenspace of $\mathbb{L}_0(k)$, we obtain a corresponding eigenspace of $\mathbb{L}$ as

$$E_\lambda(\mathbb{L}) = \{\mathbf{u}\,(\theta-\varphi)\,e^{ik(\cos\varphi,\sin\varphi)\cdot\mathbf{x}} + c.c. : \mathbf{u}(\theta) \in E_\lambda(\mathbb{L}_0), \varphi \in [0,2\pi)\}$$

which is necessarily infinite-dimensional. In order to make this eigenspace amenable to bifurcation theory, we restrict the function space to doubly periodic functions on a lattice. This consequently reduces $\mathbf{O}(2) \ltimes \mathbb{R}^2$ equivariance to $\mathbf{D}_N \ltimes \mathbf{T}^2$, where $\mathbf{D}_N$ is the holohedry of the lattice and $\mathbf{T}^2$ is the torus. Then $\varphi = 2\pi n/N$, $n = 0, ..., N-1$, where $N = 2$ for the rhombus, $N = 4$ for the square, and $N = 6$ for the hexagonal lattice. Thus $E_\lambda(\mathbb{L})$ is a $2m$, $4m$, and $6m$ dimensional space, respectively, where $m = \dim(E_\lambda(\mathbb{L}_0))$. In general $E_\lambda(\mathbb{L}_0)$ could still be infinite-dimensional. However, in the context of bifurcation theory, we look for a one-dimensional nullspace for $\mathbb{L}_0$, and hence the nullspace of $\mathbb{L}$ will be 2, 4, and 6 dimensional for rhombus, square, and hexagonal lattice respectively.

For each $\mathbf{k}$ the associated subspace of eigenfunctions

$$W_\mathbf{k} = \left\{\mathbf{u}(\theta-\varphi)\mathrm{e}^{i\mathbf{k}\cdot\mathbf{x}} + c.c\right\}, \quad \mathbf{k} = k(\cos\varphi, \sin\varphi) \tag{4.6}$$

decomposes into two $\mathbb{L}_0(k)$-invariant subspaces

$$W_\mathbf{k} = W_\mathbf{k}^+ \oplus W_\mathbf{k}^-, \tag{4.7}$$

corresponding to even (respectively, odd) functions in θ

$$W_{\mathbf{k}}^{+} = \{\mathbf{w} \in W_{\mathbf{k}} : \mathbf{u}(-\theta) = \mathbf{u}(\theta)\} = \{\mathbf{w} \in W_{\mathbf{k}} : a(-\theta) = a(\theta)\} \tag{4.8a}$$

$$W_{\mathbf{k}}^{-} = \{\mathbf{w} \in W_{\mathbf{k}} : \mathbf{u}(-\theta) = -\mathbf{u}(\theta)\} = \{\mathbf{w} \in W_{\mathbf{k}} : p = 0, a(-\theta) = -a(\theta)\}. \tag{4.8b}$$

This is a consequence of reflection symmetry of the system. Let $\kappa_{\mathbf{k}}$ denote reflections about the wavevector $\mathbf{k}$ so that $\kappa_{\mathbf{k}}\mathbf{k} = \mathbf{k}$. Then $\kappa_{\mathbf{k}}[\mathbf{u}(\theta - \varphi)e^{i\mathbf{k}\cdot\mathbf{x}}] = \mathbf{u}(\varphi - \theta)e^{i\mathbf{k}\cdot\mathbf{x}}$. Since $\kappa_{\mathbf{k}}$ is a reflection, any space that it acts on decomposes into two subspaces – one on which it acts as the identity I and one on which it acts as $-I$. Moreover, equivariance implies that $\mathbb{L}$ commutes with any reflection in $\mathbf{O}(2)$ and thus

$$\lambda\mathbf{w} = \mathbb{L}\mathbf{w} \implies \lambda[\kappa\mathbf{w}] = \mathbb{L}[\kappa\mathbf{w}],$$

which naturally leads to this particular splitting of $W_{\mathbf{k}}$. Note, however, that this does not necessarily imply that $W_{\mathbf{k}}^{+}$ and $W_{\mathbf{k}}^{-}$ have the same eigenvalues. The even and odd functions correspond to scalar and pseudoscalar representations of the Euclidean group [3, 4, 2].

4.2. Discrete velocities

Now suppose that there exists a homogeneous fixed point solution of equations (3.11) given by $P(\mathbf{x}, t) = P^s$ and $A_j(\mathbf{x}, t) = A^s$ for $j = 0, \ldots, N-1$. Linearizing about this fixed point yields the spectral problem

$$\lambda \begin{bmatrix} P \\ \mathbf{A} \end{bmatrix} = \mathbb{L} \begin{bmatrix} P \\ \mathbf{A} \end{bmatrix}$$

where $\mathbf{A} = (A_0, \ldots, A_{N-1})^{\top}$ and $\mathbb{L}$ is the linear operator on $C^2(\mathbb{R}^2, \mathbb{R}^{N+1})$ defined by

$$\mathbb{L}P \equiv \gamma(\nabla^2 + f_P)P + f_A \sum_n A_n \tag{4.9a}$$

$$\mathbb{L}A_j \equiv -\boldsymbol{\ell}_j \cdot \nabla A_j + (g_A - 1)A_j + \left(\frac{1}{N-1} + g_A\right) \sum_{n \neq j} A_n + g_P P. \tag{4.9b}$$

Again, translation symmetry implies that eigenfunctions have the form $\mathbf{u}e^{i\mathbf{k}\cdot\mathbf{x}}$ for some $\mathbf{u} \in \mathbb{C}^{N+1}$. Substituting this into equation (4.9b) yields the spectral problem

$$\lambda p = \quad (-\gamma||\mathbf{k}||^2 + f_p)p + f_A \sum a_n \tag{4.10a}$$

$$\lambda a_j = \quad -(i\boldsymbol{\ell}_j \cdot \mathbf{k} + 1 - g_A)a_j + \left(\frac{1}{N-1} + g_A\right) \sum_{n \neq j} a_n + g_p p, \tag{4.10b}$$

for $j = 0, \ldots, N-1$, which is a matrix eigenvalue problem. In the sequel, we will denote the coefficient matrix as $L(\mathbf{k})$. In contrast to the previous case, there is

no longer continuous $\mathbf{O}(2)$ symmetry, so the dispersion curves (the relationship between wavevector $\mathbf{k}$ and eigenvalue λ) and coefficients p, a_j now depend on the wave vector $\mathbf{k}$ rather than just the magnitude $||\mathbf{k}||$. Thus we cannot reduce the system as we did in equation (4.4). However, we can derive other properties that will help reduce the complexity.

First, we will derive the induced action on functions of the form

$$\mathbf{w}(\mathbf{k}) = \mathbf{u}e^{i\mathbf{k}\cdot x}, \quad \mathbf{u} = \begin{bmatrix} p \\ \mathbf{a} \end{bmatrix} \in \mathbb{C}^{N+1},$$

where $\mathbf{a} = (a_0, \dots, a_{N-1})^\top$. Here translation simply acts as multiplication since

$$\sigma\mathbf{w}(\mathbf{k}) = \mathbf{u}e^{i\mathbf{k}\cdot(\mathbf{x}-\mathbf{x}_0)} = e^{-i\mathbf{k}\cdot\mathbf{x}_0}\mathbf{u}e^{i\mathbf{k}\cdot\mathbf{x}} = e^{-i\mathbf{k}\cdot\mathbf{x}_0}\mathbf{w}(\mathbf{k}) \quad \forall \mathbf{x}_0 \in \mathbb{R}^2.$$

For $\sigma \in \mathbf{D}_N$, we have the induced action

$$\sigma\mathbf{w}(\mathbf{k}) = \sigma[\mathbf{u}e^{i\mathbf{k}\cdot\mathbf{x}}] = [\mathbb{P}_\sigma^{-1}\mathbf{u}]e^{i\mathbf{k}\cdot(\sigma^{-1}\mathbf{x})} = [\mathbb{P}_\sigma^{-1}\mathbf{u}]e^{i(\sigma\mathbf{k})\cdot\mathbf{x}} = \mathbb{P}_\sigma^{-1}\mathbf{w}(\sigma\mathbf{k})$$

where $\mathbb{P}_\sigma$ is the permutation matrix corresponding to the group element σ defined in equation (3.16). Similarly, we have the induced action

$$\sigma[L(\mathbf{k})\mathbf{w}(\mathbf{k})] = \mathbb{P}_\sigma^{-1}L(\sigma\mathbf{k})\mathbf{w}(\sigma\mathbf{k}) = L(\mathbf{k})\mathbb{P}_\sigma^{-1}\mathbf{w}(\sigma\mathbf{k}) = L(\mathbf{k})[\sigma\mathbf{w}(\mathbf{k})],$$

where the last expression follows from equivariance. We thus have the identity

$$L(\sigma\mathbf{k}) = \mathbb{P}_\sigma L(\mathbf{k})\mathbb{P}_\sigma^{-1}, \quad \forall\sigma \in \mathbf{D}_N. \tag{4.11}$$

Using this identity, we can infer some details about the structure of the eigenspaces of $L(\mathbf{k})$.

Lemma 4.1. *If $\{\lambda, \mathbf{u}\}$ is an eigenpair of $L(\mathbf{k})$ then $\{\lambda, \mathbb{P}_\sigma\mathbf{u}\}$ is an eigenpair of $L(\sigma\mathbf{k})$.*

Proof. The proof follows from

$$L(\sigma\mathbf{k})\mathbb{P}_\sigma\mathbf{u} = \mathbb{P}_\sigma L(\mathbf{k})\mathbb{P}_\sigma^{-1}\mathbb{P}_\sigma\mathbf{u} = \mathbb{P}_\sigma L(\mathbf{k})\mathbf{u} = \lambda\mathbb{P}_\sigma\mathbf{u}.$$

Proposition 4.3. *Both $\{\lambda, \mathbf{u}\}$ and $\{\overline{\lambda}, \mathbb{P}_\pi^{-1}\overline{\mathbf{u}}\}$ are eigenpairs of $L(\mathbf{k})$.*

Proof. Suppose that $\{\lambda, \mathbf{u}\}$ is an eigenpair of $L(\mathbf{k})$ for a fixed $\mathbf{k}$. Conjugating the solutions

$$\mathbf{u}e^{\lambda t + i\mathbf{k}\cdot\mathbf{x}}$$

of the time-dependent linearized equation reveals that $\{\overline{\lambda}, \overline{\mathbf{u}}\}$ must be an eigenpair of $L(-\mathbf{k})$. Since $R_\pi\mathbf{k} = -\mathbf{k}$ for all $\mathbf{k}$, it follows from equation (4.11) that

$$\overline{L}(\mathbf{k}) = L(-\mathbf{k}) = L(R_\pi\mathbf{k}) = \mathbb{P}_\pi L(\mathbf{k})\mathbb{P}_\pi^{-1},$$

and therefore

$$\overline{L}(\mathbf{k})\overline{\mathbf{u}} = \overline{\lambda}\overline{\mathbf{u}} \implies L(\mathbf{k})\mathbb{P}_\pi^{-1}\overline{\mathbf{u}} = \overline{\lambda}\mathbb{P}_\pi^{-1}\overline{\mathbf{u}}.$$

Although $L(\mathbf{k})$ shares the property of real-valued matrices that eigenvalues always come in conjugate pairs, the eigenvectors do not have this property: the conjugate of the eigenvector must be accompanied by an appropriate permutation. As the system has an odd number of eigenvalues (since the matrix has an odd size), there must be an odd number of real eigenvalues. We are particularly interested in the existence of a zero eigenvalue with multiplicity 1, since this corresponds to a local codimension one bifurcation. In this case, the following corollary describes the form of the null vector.

Corollary 4.5. *If λ is a real eigenvalue with multiplicity 1, then its eigenvector has the form*

$$\mathbf{u} = \begin{bmatrix} p \\ a_0 \\ \vdots \\ a_{N/2-1} \\ \overline{a}_0 \\ \vdots \\ \overline{a}_{N/2-1} \end{bmatrix}$$

with $p \in \mathbb{R}$.

Proof. By proposition 5.2, if λ is real then $\mathbf{u}$ and $\mathbb{P}_\pi^{-1}\overline{\mathbf{u}}$ are both its corresponding eigenvectors. Hence, if the eigenspace is one dimensional, they must be equal (up to a constant multiple). Since $\mathbb{P}_\pi^{-1} a_j = a_{j-N/2} \pmod N$ for $j = 1, ..., N$, then the components of $\mathbf{u}$ must satisfy $a_{j+N/2} = \overline{a}_j$ for $j = 0, ..., N/2-1$. Moreover, with this choice, all terms in the first equation of (4.10) are real and hence p must be real.

The consequence of this corollary is the following. In a Turing bifurcation, we seek a single real eigenvalue crossing the imaginary axis and hence we require a one dimensional eigenspace for that real eigenvalue. In particular, at bifurcation, the null vector must have the form given in Corollary 4.5 and this will greatly reduce the complexity of subsequent analysis in later sections.

Next, to reduce the complexity further, analogous to the isotropic case, define

$$W_{\mathbf{k}} = \{\mathbf{u}e^{i\mathbf{k}\cdot\mathbf{x}} + c.c.\}.$$

In general, it is not possible to form the decomposition $W_{\mathbf{k}} = W_{\mathbf{k}}^+ \oplus W_{\mathbf{k}}^-$ as in the isotropic case. This is due to the fact that reflections such that $\kappa\mathbf{k} = \mathbf{k}$ do not exist in $\mathbf{D}_N$ unless $\mathbf{k}$ is along an axis of reflection for the polygon, in which case

$$\mathbf{k} = k(\pm 1, 0), \quad k(0, \pm 1), \quad k(\pm 1, \pm 1)$$

for square

$$\mathbf{k} = k(\pm 1, 0), \quad k(0, \pm 1), \quad k(\pm 1/2, \pm\sqrt{3}/2)$$

for hexagonal. In terms of Turing bifurcation, we are only concerned with those $\mathbf{k}$ such that the largest eigenvalue $\lambda(\mathbf{k})$ of $L(\mathbf{k})$ is real and crosses zero

as the parameter value γ changes. We are unable to determine analytically the direction for $\mathbf{k}$ yielding the largest eigenvalue. However, we numerically compute the eigenvalues of $L(\mathbf{k})$ for various $f_P, f_A, g_P, g_A, \gamma$ within the range reported by [9] and observe that the largest eigenvalue occurs for wavevectors of the form

$$\mathbf{k} = \begin{cases} k(\boldsymbol{\ell}_1 + \boldsymbol{\ell}_2) = k(1,1), & N = 4 \\ k(\boldsymbol{\ell}_1 + \boldsymbol{\ell}_3) = \frac{k}{2}(1, \sqrt{3}), & N = 6 \end{cases} \tag{4.12}$$

as well as, due to symmetry, rotations and reflections in $\mathbf{D}_N$ of those wavevectors. See Fig. 4 for an example. Note that we could set $\mathbf{k} = k(1,0)$ in the hexagonal case, which coincides with the choice for systems with $\mathbf{O}(2)$ symmetry. However, instead, we choose the form in equation (4.12), so that it looks analogous to the square case.

Given the above choice, we perform the decomposition $W_{\mathbf{k}} = W_{\mathbf{k}}^+ \oplus W_{\mathbf{k}}^-$ where

$$W_{\mathbf{k}}^+ = \{\mathbf{w} \in W_{\mathbf{k}} : \mathbb{P}_{\kappa_{\mathbf{k}}}^{-1}\mathbf{u} = \mathbf{u}\}, \quad W_{\mathbf{k}}^- = \{\mathbf{w} \in W_{\mathbf{k}} : \mathbb{P}_{\kappa_{\mathbf{k}}}^{-1}\mathbf{u} = -\mathbf{u}\}$$

and $\kappa_{\mathbf{k}}$ is the reflection, in the scalar representation, across the axis spanned by $\mathbf{k}$. Denoting $\mathbf{u} = (p, a_0, ..., a_{N-1})^T$, observe that

$$\kappa_{\mathbf{k}} \begin{bmatrix} p \\ a_0 \\ a_1 \\ a_2 \\ a_3 \end{bmatrix} = \begin{bmatrix} p \\ a_1 \\ a_0 \\ a_3 \\ a_2 \end{bmatrix} \quad \text{for } N = 4, \qquad \kappa_{\mathbf{k}} \begin{bmatrix} p \\ a_0 \\ a_1 \\ a_2 \\ a_3 \\ a_4 \\ a_5 \end{bmatrix} = \begin{bmatrix} p \\ a_2 \\ a_1 \\ a_0 \\ a_5 \\ a_4 \\ a_3 \end{bmatrix} \quad \text{for } N = 6$$

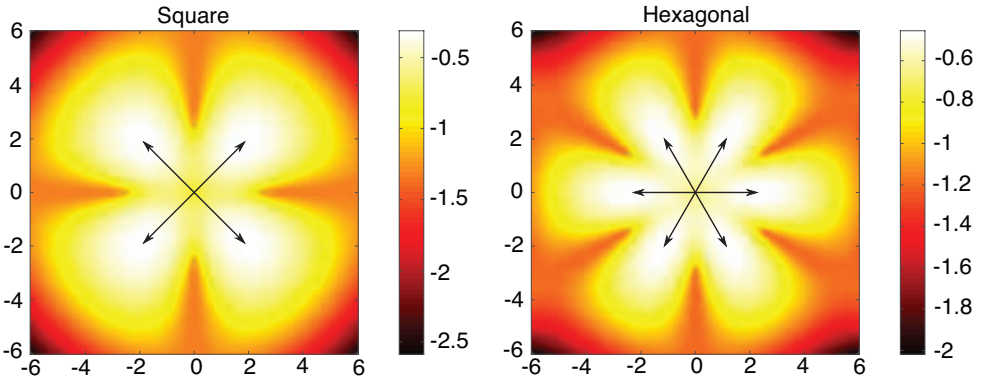

Figure 4: Density plots of the maximum eigenvalues of $L(\mathbf{k})$ as a function of the wavevector $\mathbf{k} \in \mathbb{R}^2$. Black arrows indicate the direction for $\mathbf{k}$ yielding the largest eigenvalue. Parameter values are $f_A = -0.1625, f_P = 0.8, g_A = -1.1, g_P = 8.8, \gamma = 0.005$.

and hence

$$W_{\mathbf{k}}^{S,+} = \left\{ \begin{bmatrix} p \\ a \\ a \\ b \\ b \end{bmatrix} e^{i\mathbf{k}\cdot\mathbf{x}} + c.c. : p, a, b \in \mathbb{C} \right\}, \quad W_{\mathbf{k}}^{S,-} \left\{ \begin{bmatrix} 0 \\ a \\ -a \\ b \\ -b \end{bmatrix} e^{i\mathbf{k}\cdot\mathbf{x}} + c.c. : a, b \in \mathbb{C} \right\}$$

for $N = 4$ and

$$W_{\mathbf{k}}^{H,+} = \left\{ \begin{bmatrix} p \\ a \\ b \\ a \\ c \\ d \\ c \end{bmatrix} e^{i\mathbf{k}\cdot\mathbf{x}} + c.c. : p, a, b, c, d \in \mathbb{C} \right\}, \quad W_{\mathbf{k}}^{H,-} \left\{ \begin{bmatrix} 0 \\ a \\ 0 \\ -a \\ c \\ 0 \\ -c \end{bmatrix} e^{i\mathbf{k}\cdot\mathbf{x}} + c.c. : a, c \in \mathbb{C} \right\}$$

for $N = 6$. Let $V^{S/H,\pm} \subset \mathbb{C}^{N+1}$ be the subspaces of vectors corresponding to $W_{\mathbf{k}}^{S/H,\pm}$. By corollary 4.5, if the nullspace at $\mathbf{k} = \mathbf{k}_c$ is one dimensional then these subspaces take the reduced form

$$W_{\mathbf{k}_c}^{S,+} = \left\{ \begin{bmatrix} p \\ a \\ a \\ \overline{a} \\ \overline{a} \end{bmatrix} e^{i\mathbf{k}_c\cdot\mathbf{x}} + c.c. : p \in \mathbb{R}, a \in \mathbb{C} \right\} \quad \text{or} \quad W_{\mathbf{k}_c}^{S,-} = \left\{ \begin{bmatrix} 0 \\ a \\ -a \\ \overline{a} \\ -\overline{a} \end{bmatrix} e^{i\mathbf{k}_c\cdot\mathbf{x}} + c.c. : a \in \mathbb{C} \right\}$$

for $N = 4$ and

$$W_{\mathbf{k}_c}^{H,+} = \left\{ \begin{bmatrix} p \\ a \\ b \\ a \\ \overline{a} \\ \overline{b} \\ \overline{a} \end{bmatrix} e^{i\mathbf{k}_c\cdot\mathbf{x}} + c.c. : a, b \in \mathbb{C} \right\} \quad \text{or} \quad W_{\mathbf{k}_c}^{H,-} \left\{ \begin{bmatrix} 0 \\ a \\ 0 \\ -a \\ \overline{a} \\ 0 \\ -\overline{a} \end{bmatrix} e^{i\mathbf{k}_c\cdot\mathbf{x}} + c.c. : p \in \mathbb{R}, a \in \mathbb{C} \right\}$$

for $N = 6$ depending on the subspace $V^{S/H,\pm}$ in which $\mathbf{u}$ resides.

Finally, restricting the form of $\mathbf{k}$ as described above, reduces the eigenvalue problem to

$$\lambda p = \quad (-2\gamma k^2 + f_p)p + f_A \sum a_n \tag{4.13a}$$

$$\lambda a_j = \quad -(ik + 1 - g_A)a_j + \left(\frac{1}{3} + g_A\right) \sum_{n \neq j} a_n + g_p p, \quad j = 0, 1 \tag{4.13b}$$

$$\lambda a_j = \quad -(-ik + 1 - g_A)a_j + \left(\frac{1}{3} + g_A\right) \sum_{n \neq j} a_n + g_p p, \quad j = 2, 3 \tag{4.13c}$$

for $N = 4$ and

$$\lambda p = (-\gamma k^2 + f_p)p + f_A \sum a_n \tag{4.14a}$$

$$\lambda a_j = -\left(i\frac{k}{2} + 1 - g_A\right) a_j + \left(\frac{1}{5} + g_A\right) \sum_{n \neq j} a_n + g_p p, \quad j = 0, 2 \tag{4.14b}$$

$$\lambda a_1 = -\left(ik + 1 - g_A\right) a_j + \left(\frac{1}{5} + g_A\right) \sum_{n \neq j} a_n + g_p p, \tag{4.14c}$$

$$\lambda a_j = -\left(-i\frac{k}{2} + 1 - g_A\right) a_1 + \left(\frac{1}{5} + g_A\right) \sum_{n \neq j} a_n + g_p p, \quad j = 3, 5 \tag{4.14d}$$

$$\lambda a_4 = -\left(-ik + 1 - g_A\right) a_4 + \left(\frac{1}{5} + g_A\right) \sum_{n \neq j} a_n + g_p p, \tag{4.14e}$$

for $N = 6$. We will write these eigenvalue equations in the more compact form

$$\lambda \begin{bmatrix} p \\ \mathbf{a} \end{bmatrix} = L_0^{S/H}(k) \begin{bmatrix} p \\ \mathbf{a} \end{bmatrix}, \tag{4.15}$$

where $L_0^S(k)$ and $L_0^H(k)$ are the matrix operators on the square and hexagonal lattices, respectively.

4.3. Stability to spatially homogeneous perturbations

We now derive conditions for stability with respect to spatially uniform perturbations for both the isotropic and discrete velocity models, which is a necessary condition for the occurrence of a Turing bifurcation. We summarize these results in the following proposition.

Proposition 4.7. *Define*

$$\beta_\Omega = f_P + \Omega g_A, \quad \delta = f_P g_A - f_A g_P$$

where $\Omega = 2\pi$ for the isotropic case and $\Omega = N$ for the discrete case. The fixed point of equation (3.5) is stable with respect to spatially uniform perturbations if and only if $\beta_\Omega < 0$ and $\delta > 0$.

Proof. Proof in Appendix A.1

4.4. Turing bifurcations

Suppose that the conditions of proposition 4.7 hold. The next step in establishing the occurrence of a Turing bifurcation is to show that there exists a critical value of the bifurcation parameter, $\gamma = \gamma_c$, a critical wavenumber $k = k_c \neq 0$ and a single real branch of eigenvalues for which $\lambda(k_c) = 0$. We show this explicitly in the isotropic case (section 5) and in the discrete case on

a square lattice (section 6). However, we have not been able to establish the existence of a critical bifurcation point for discrete velocities on a hexagonal lattice, and so we will not consider this case further. A Turing bifurcation will then occur if this real branch (dispersion curve) crosses the k-axis from below as γ crosses the critical point from above (transversality), assuming that the real parts of all other solution branches remain below the k-axis. This means that the homogeneous fixed point is stable for $\gamma > \gamma_c$, is marginally stable for $\gamma = \gamma_c$, and is unstable with respect to a band of modes around $k = k_c$ when $\gamma < \gamma_c$. We are only able to establish the transversality condition for the square lattice, see section 6.

Restriction of the original infinite-dimensional system to the finite-dimensional null-space of marginally stable modes, (after imposing double-periodicity in the case of isotropic velocities), means that we can then use the equivariant branching lemma [14, 25, 13, 18] to explicitly determine the planforms that would emerge through a Turing bifurcation, assuming such a bifurcation occurs. In particular, they are given by group orbits of the one-dimensional nullspace of $\mathbb{L}_0(k)$ in the isotropic case and the nullspace of $L_0^S(k)$ in the discrete case on a square lattice. For completeness, we restate the equivariant branching lemma here.

Lemma 4.9 (Equivariant branching lemma.). *Suppose that u_0 is a an equilibrium of a finite-dimensional dynamical system $\partial_t u = G(u)$. Let Σ be a subgroup of a compact Lie group Γ, where the system is Γ equivariant. Define the fixed point subspace*

$$Fix(\Sigma) = \{u \in null(\mathbb{L}) | \sigma u = u, \forall \sigma \in \Sigma\}.$$

Then for each Σ with $dim(Fix(\Sigma)) = 1$, there exists a unique equilibrium solution branch bifurcating from $u = u_0$, such that the bifurcating solutions have symmetry Σ.

5. Planforms for isotropic velocities

5.1. Marginal stability

In the isotropic case we need to determine the nullspace of the linear operator $\mathbb{L}_0(k)$ defined by equations (4.4). We first show that there are no eigenfunctions in the subspace $W_{\mathbf{k}}^-$. Suppose $(p, a(\theta)) \in W_{\mathbf{k}}^-$, which implies that $a(\theta)$ is odd and thus $\int a(\theta) = 0$. Then equation (4.4) becomes

$$\begin{aligned} \lambda p &= (-\gamma k^2 + f_P)p \\ \lambda a(\theta) &= g_P p - (ik\cos(\theta) + 1)a(\theta). \end{aligned}$$

The second equation implies that

$$p = \frac{1}{g_P}(ik\cos(\theta) + 1 + \lambda)a(\theta).$$

Since p is constant in θ, this can hold only if

$$a(\theta) \propto \frac{1}{ik\cos(\theta) + 1 + \lambda}$$

which contradicts $a(\theta)$ being odd. Note that p must be non-zero, since otherwise we would have $a(\theta) = 0$. Therefore $(p, a(\theta))$ cannot be an element of the nullspace when $a(\theta)$ is odd. In fact, this same argument shows that elements of the nullspace must satisfy $\int a(\theta) \neq 0$ whether $a(\theta)$ is odd or even. This means $a(\theta)$ must have a constant term in its Fourier series.

For $(p, a(\theta)) \in W_{\mathbf{k}}^{+}$ we can derive a dispersion relation between the eigenvalues λ and wavenumber $\mathbf{k}$, which we present in the following proposition.

Proposition 5.1. *For each $k \in \mathbb{R}$ the corresponding eigenvalues are the zeros of*

$$d(\lambda, k) = (\lambda + \gamma k^2 - f_P)\left[((\lambda+1)^2 + k^2)^{1/2} - (1 + 2\pi g_A)\right] - 2\pi f_A g_P \quad (5.1)$$

for all

$$\lambda \neq -1 \pm \sqrt{(1+2\pi g_A)^2 - k^2}, -1 \pm ik\cos(\varphi) \quad \varphi \in [0, 2\pi).$$

Here we define $((\lambda+1)^2 + k^2)^{1/2}$ with branch cut between $-1-ik$ and $-1+ik$ with values positive for real values of $\lambda > -1$ and negative for real values of $\lambda < -1$. Additionally, for each eigenvalue λ and wavenumber k, the corresponding eigenfunction is $(1, a(\theta))$ with

$$a(\theta) = \frac{\lambda + \gamma k^2 - f_P}{2\pi f_A h(\lambda, k)} \frac{1 + \overline{\lambda} - ik\cos(\theta)}{(Re(\lambda)+1)^2 + (Im(\lambda) + k\cos(\theta))^2}$$

and

$$h(\lambda, k) = \left((1+\lambda)^2 + k^2\right)^{-1/2}$$

Proof. Proof in Appendix A.2.

Therefore, setting $\lambda = 0$ in the dispersion relation (5.1) implies that $\mathbb{L}_0(k)$ has a nullspace only if k is a solution of

$$0 = (\gamma k^2 - f_P)(\sqrt{1+k^2} - 1) - 2\pi\gamma g_A k^2 + 2\pi\delta. \quad (5.2)$$

Moreover, by proposition 5.1, as long as $\sqrt{1+k^2} \neq 1 + 2\pi g_A$ then the nullspace is necessarily one dimensional (for fixed k). It remains to find sufficient conditions for a 1D nullspace to exist at a single $k = k_c > 0$ for some $\gamma = \gamma_c$. These are stated in the following proposition.

Proposition 5.3. *Suppose that the conditions in proposition 4.7 hold and f_P, g_A are opposite in sign. If $g_A < 0$ and $f_P > 0$ then there exists a γ_c such that*

(a) If $\gamma > \gamma_c$ then $\mathbb{L}_0(k)$ is non-singular for all k.

(b) If $\gamma = \gamma_c$ then $\mathbb{L}_0(k)$ has exactly one zero eigenvalue for some $k = k_c$ with corresponding nullvector $(1, a(\theta))$, where

$$a(\theta) = \frac{(\gamma_c k_c^2 - f_P)\sqrt{1+k_c^2}}{2\pi f_A} \frac{1 - ik_c\cos(\theta)}{k_c^2\cos^2(\theta)+1},$$

and is non-singular for all $k \neq k_c$.

(c) If $\gamma < \gamma_c$ (sufficiently close) then $\mathbb{L}_0(k)$ has one zero eigenvalue for two values of $k > 0$ and is non-singular elsewhere.

If $g_A > 0$ and $f_P < 0$ then the inequalities in (a) and (c) are reversed.

PROOF. Proof in Appendix A.3

5.2. Group actions and doubly periodic planforms

We will now find all the one-dimensional fixed point subspaces in order to apply the equivariant branching lemma. First, using the nullspaces for $\mathbb{L}_0(k)$ we apply symmetry to obtain the nullspace of the full operator $\mathbb{L}$. Note that, in the isotropic case, we obtain a finite-dimensional space by restricting $\mathbb{L}$ to doubly periodic functions on the square and hexagonal lattice. (On the other hand, such a restriction is not required in the discrete case, since the eigenfunctions are doubly periodic due to the intrinsic structure of the model.)

Theorem 5.5. *In the space of doubly-periodic functions on the lattice $\mathcal{L}$, the nullspace of the operator $\mathbb{L}$ in equation (4.1), at $\gamma = \gamma_c$, is given by*

$$null(\mathbb{L}) = \left\{ z_1 \mathbf{u}(\theta) e^{i\mathbf{k}_1\cdot\mathbf{x}} + z_2 \mathbf{u}\left(\theta - \frac{\pi}{2}\right) e^{i\mathbf{k}_2\cdot\mathbf{x}} + c.c. \right\} \cong \mathbb{C}^2$$

for $\mathcal{L}$ a square lattice and

$$null(\mathbb{L}) = \left\{ z_1 \mathbf{u}(\theta) e^{i\mathbf{k}_1\cdot\mathbf{x}} + z_2 \mathbf{u}\left(\theta - \frac{2\pi}{3}\right) e^{i\mathbf{k}_2\cdot\mathbf{x}} + z_3 \mathbf{u}\left(\theta + \frac{2\pi}{3}\right) e^{i\mathbf{k}_3\cdot\mathbf{x}} + c.c. \right\} \cong \mathbb{C}^3$$

for $\mathcal{L}$ a hexagonal lattice. The wavevectors are

$$\mathbf{k}_1 = k_c(1,0), \quad \mathbf{k}_2 = k_c(0,1)$$

for square and

$$\mathbf{k}_1 = k_c(1,0), \quad \mathbf{k}_2 = \frac{k_c}{2}(-1,\sqrt{3}), \quad \mathbf{k}_3 = -(\mathbf{k}_1+\mathbf{k}_2) = -\frac{k_c}{2}(1,\sqrt{3})$$

for hexagonal. The vector-valued function $\mathbf{u}(\theta)$ is of the form

$$\mathbf{u}(\theta) = \begin{bmatrix} 1 \\ a(\theta) \end{bmatrix},$$

where $a(\theta)$ is defined in proposition 5.3.

PROOF. The proof follows from proposition 5.3 and $\mathbf{D}_N \ltimes \mathbf{T}^2$ equivariance.

We must now determine how the group action affects the entries z_n of vectors of $\mathbb{C}^N$. We proceed by computing the actions from the generators $\kappa_{\mathbf{k}_c}$ (reflection about the line spanned by $\mathbf{k}_c$) and $R_{2\pi/N}$, as well as elements in the torus, which we will denote as $[s,t] \in \mathbf{T}^2$. The actions are the same between the isotropic velocities and discrete velocities case. A simple calculation shows that

$$\kappa(z_1, z_2) = \pm(z_1, \overline{z}_2) \tag{5.3a}$$
$$R_{\pi/2}(z_1, z_2) = (\overline{z}_2, z_1) \tag{5.3b}$$
$$[s,t](z_1, z_2) = (e^{-is} z_1, e^{-it} z_2). \tag{5.3c}$$

for $N = 4$ and

$$\kappa(z_1, z_2, z_3) = \pm(z_1, z_3, z_2) \tag{5.4a}$$
$$R_{\pi/3}(z_1, z_2, z_3) = (\overline{z_2}, \overline{z_3}, \overline{z_1}) \tag{5.4b}$$
$$[s,t](z_1, z_2, z_3) = (e^{-is} z_1, e^{-it} z_2, e^{i(s+t)} z_3). \tag{5.4c}$$

for $N = 6$. The third element of the mapping for $[s,t]$ arises from the choice $\mathbf{k}_3 = -(\mathbf{k}_1 + \mathbf{k}_2)$. For reflections, the $+$ indicates scalar actions while $-$ indicatespseudoscalar actions. For a proof see [4].

Equations (5.3) and (5.4) describe standard actions on $\mathbb{C}^{N/2}$. The one-dimensional fixed point subspaces have been found in [4], which we summarize in the following proposition.

Proposition 5.7. *The one-dimensional fixed point subspaces along with their isotropy subgroups are given in the tables below for both the scalar and pseudoscalar action, . Here* $\xi = \frac{2\pi}{N}$, $\mathbf{D}_m(\sigma_1, \sigma_2)$ *are the dihedral groups generated by* σ_1 *and* σ_2, $\mathbb{Z}_m(\sigma)$ *are the cyclic groups generated by* σ *and* $\mathbf{S}^1$ *is generated by* $[0,t] \in \mathbf{T}^2$.

Scalar Representation			
Lattice	*Pattern*	*Isotropy Subgroup*	*Fixed Point*
Square	*Esquare*	$\mathbf{D}_4(\kappa_{\mathbf{k}}, \xi)$	$(1,1)$
	Eroll	$\mathbb{Z}_2(\kappa_{\mathbf{k}}) \oplus \mathbf{S}^1$	$(1,0)$
Hexagonal	*EhexagonP*	$\mathbf{D}_6$	$(1,1,1)$
	EhexagonM	$\mathbf{D}_6$	$(-1,-1,-1)$
	Eroll	$\mathbb{Z}_2(\kappa_{\mathbf{k}}) \oplus \mathbf{S}^1$	$(1,0,0)$

Pseudocalar Representation			
Lattice	*Pattern*	*Isotropy Subgroup*	*Fixed Point*
Square	*Osquare*	$\mathbf{D}_4(\kappa_{\mathbf{k}}[1/2,1/2], \xi)$	$(1,1)$
	Oroll	$\mathbb{Z}_2(\xi^2 \kappa_{\mathbf{k}}[1/2,0]) \oplus \mathbf{S}^1$	$(1,0)$
Hexagonal	*Ohexagon*	$\mathbb{Z}_6(\xi)$	$(1,1,1)$
	Otriangle	$\mathbf{D}_3(\kappa_{\mathbf{k}}\xi, \xi^2)$	(i,i,i)
	Orectangle	$\mathbf{D}_2(\kappa_{\mathbf{k}}, \xi^3)$	$(0,1,-1)$
	Oroll	$\mathbb{Z}_4(\xi^3 \kappa_{\mathbf{k}}[1/2,0]) \oplus \mathbf{S}^1$	$(1,0,0)$

For the hexagonal lattice with the scalar representation, the fixed points $(1,1,1)$ and $(-1,-1,-1)$ have the same isotropy subgroup. However, they are not on the same group orbit and thus generate distinct patterns. This is in contrast to the pseudoscalar case, where reflections also multiply by -1 and these two points are on the same group orbit.

We can now use the equivariant branching lemma [14] to determine the solutions emerging from the Turing bifurcations. Keep in mind that the pseudoscalar solutions are only guaranteed to exists when f and g are odd, whereas the scalar solutions are always guaranteed.

Theorem 5.8. *Suppose that the uniform fixed point of equation (3.7) undergoes a Turing bifurcation at some parameter $\gamma = \gamma_c$. Then for each isotropy subgroup Σ in proposition 5.7, there exists a branch of solutions bifurcating from the uniform fixed point with symmetry group Σ.*

Combining theorems 5.3 and 5.5 we see that the planforms are given by

$$\begin{bmatrix} P(\mathbf{x}) \\ A(\mathbf{x},\theta) \end{bmatrix} = z_1 \begin{bmatrix} 1 \\ a(\theta) \end{bmatrix} e^{ik_c x} + z_2 \begin{bmatrix} 1 \\ a\left(\theta - \frac{\pi}{2}\right) \end{bmatrix} e^{ik_c y} + c.c.$$

for a square lattice and

$$\begin{aligned} \begin{bmatrix} P(\mathbf{x}) \\ A(\mathbf{x},\theta) \end{bmatrix} = z_1 \begin{bmatrix} 1 \\ a(\theta) \end{bmatrix} e^{ik_c x} + z_2 \begin{bmatrix} 1 \\ a\left(\theta - \frac{2\pi}{3}\right) \end{bmatrix} e^{i\frac{k_c}{2}(-x+\sqrt{3}y)} \\ + z_3 \begin{bmatrix} 1 \\ a\left(\theta + \frac{2\pi}{3}\right) \end{bmatrix} e^{i\frac{k_c}{2}(-x-\sqrt{3}y)} + c.c. \end{aligned}$$

for a hexagonal lattice, where

$$a(\theta) = \frac{(\gamma_c k_c^2 - f_P)\sqrt{1+k_c^2}}{2\pi f_A} \frac{1 - ik_c\cos(\theta)}{k_c^2\cos^2(\theta)+1}.$$

The values of z_1, z_2, z_3 depend on the isotropy subgroup according to proposition 5.7.

Note that the total concentration of AT particles is

$$\mathcal{A}(\mathbf{x}) = \int A(\mathbf{x},\theta)d\theta = \frac{\gamma_c k_c^2 - f_p}{f_A} P(\mathbf{x})$$

and thus is a multiple of the concentration of PT particles. In particular the patterns are in phase if the constant is positive and antiphase if it is negative. Using the equality in equation (A.4), we see that

$$\gamma_c k_c^2 - f_P = \frac{2\pi f_A g_P}{\sqrt{1+k_c^2} - (1+2\pi g_A)} < 0$$

since $f_A g_P < 0$ and $g_A < 0$. Thus $\mathcal{A}$ and P are in phase if $f_A < 0$ and antiphase if $f_A > 0$.

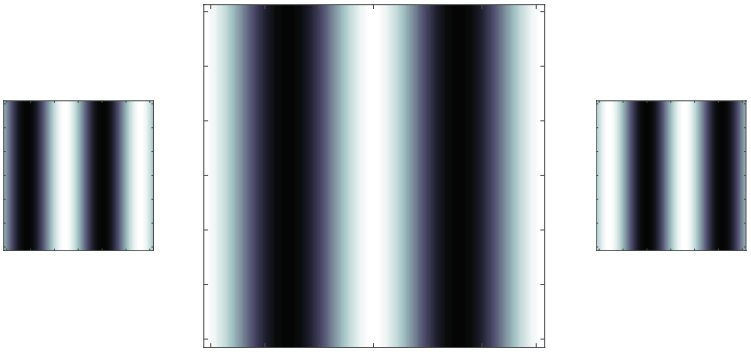

Figure 5: Density plots for $P(\mathbf{x})$ (middle) and $A(\mathbf{x},\theta)$ for $\theta = 0$ (right) and $\theta = \pi$ (left). We set $k_c = 2$ as any other value yields qualitatively similar plots.

We will now analyze the individual concentrations $A(\mathbf{x},\theta)$. In the following we set

$$\phi(\theta) = -\frac{1}{k_c}\arg(a(\theta)) = -\frac{1}{k_c}\arg(1 - ik_c\cos(\theta))$$

and note that $|a(\theta)| = r$ is constant. Then, near bifurcation, solutions have the following forms up to a real constant multiple.

1. Rolls: Setting $(z_1, z_2) = (1, 0)$ yields

$$P(\mathbf{x}) = \cos(k_c x) \quad \text{and} \quad a(\mathbf{x},\theta) = rP(\mathbf{x} - (\phi(\theta), 0)).$$

   Up to a constant multiple, $a(\mathbf{x},\theta)$ is a translated version of $P(\mathbf{x})$ along the x-axis. Note that $\phi(\theta - \pi) = -\phi(\theta)$ and that $A(\mathbf{x},\theta - \pi)$ corresponds to particles moving in the opposite direction of $A(\mathbf{x},\theta)$. Hence, the shift is in opposing directions for particles moving in opposite directions. Moreover the shift is positive for θ corresponding to x positive and negative otherwise. This means that right-moving particles shift $P(\mathbf{x})$ to the right, while left-moving particles shift $P(\mathbf{x})$ to the left. In Fig. 5 we show plots of $P(\mathbf{x})$ along with $A(\mathbf{x},\theta)$ for $\theta = 0, \pi$ corresponding to right- and left-moving particles respectively.

2. Squares: Setting $(z_1, z_2) = (1, 1)$ yields

$$P(\mathbf{x}) = \cos(k_c x) + \cos(k_c y) \quad \text{and} \quad a(\mathbf{x},\theta) = rP(\mathbf{x} + (\phi(\theta), \phi(\theta - \pi/2))).$$

   Again, we see that $a(\mathbf{x},\theta)$ is a translated version of $P(\mathbf{x})$. In this case shifts are in both the x and y directions. As in the rolls case, we see that

$$(\phi(\theta - \pi), \phi(\theta - \pi - \pi/2)) = -(\phi(\theta), \phi(\theta - \pi/2))$$

   and the shifts are in opposing directions for AT particles moving in opposite directions.. Consider the AT particles moving along the x and

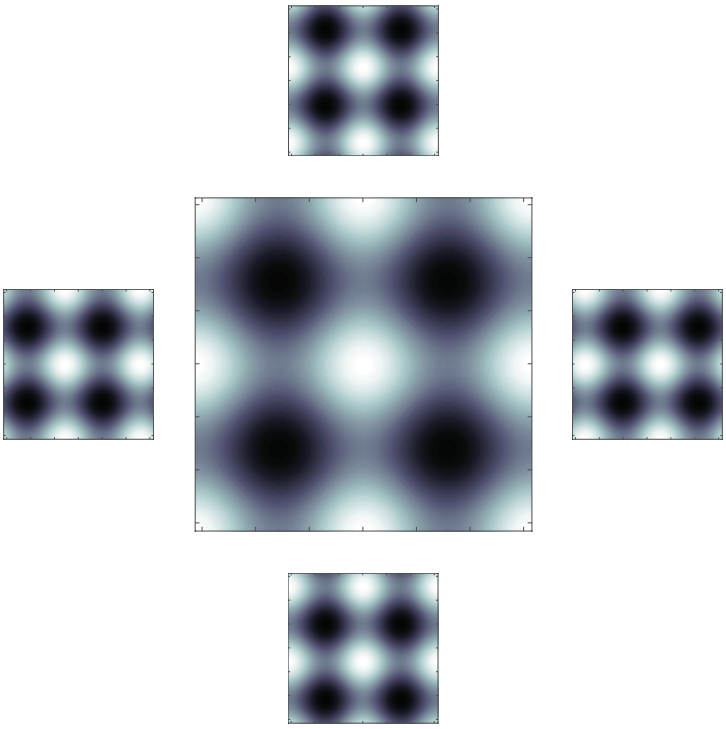

Figure 6: Density plots for square solutions with $\theta = 0, \pi/2, 3\pi/2$ and $A(\mathbf{x}, \theta)$ are arranged in those corresponding positions.

y directions $A(\mathbf{x}, 0), A(\mathbf{x}, \pi/2), A(\mathbf{x}, \pi)$, and $A(\mathbf{x}, 3\pi/2)$. The translation vectors are $(\phi_0, 0), (0, \phi_0), (0, -\phi_0)$, and $(-\phi_0, 0)$, respectively, where

$$\phi_0 = \phi(0) = -\frac{1}{k_c} \arg(1 - k_c) > 0.$$

Hence the left/right moving particles shift $P(\mathbf{x})$ to the left/right respectively, while up/down moving particles shift $P(\mathbf{x})$ up/down respectively. Other values of θ are more difficult to analyze, but we observe in our simulations that the translation vector $(\phi(\theta), \phi(\theta - \pi/2))$ traces out a closed loop. However, the length of the vector is not constant, so the loop is not a circle. In Fig. 6 we show $P(\mathbf{x})$ along with $A(\mathbf{x}, \theta)$ for $\theta = 0, \pi/2, \pi, 3\pi/2$ corresponding to right, up, left, and downward moving particles respectively.

3. Hexagons/Triangles: For hexagonal patterns we set $(z_1, z_2, z_3) = \pm(1, 1, 1)$ to obtain

$$\begin{bmatrix} P(\mathbf{x}) \\ A(\mathbf{x}, \theta) \end{bmatrix} = \begin{bmatrix} C(x) + C\left(-\frac{x}{2} + \frac{\sqrt{3}y}{2}\right) + C\left(-\frac{x}{2} - \frac{\sqrt{3}y}{2}\right) \\ r\left(C(x + \phi(\theta)) + C_+\left(-\frac{x}{2} + \frac{\sqrt{3}y}{2}, \theta\right) + C_-\left(-\frac{x}{2} - \frac{\sqrt{3}y}{2}, \theta\right)\right) \end{bmatrix},$$

while setting $(z_1, z_2, z_3) = (i, i, i)$ yields triangular patterns of the form

$$\begin{bmatrix} P(\mathbf{x}) \\ A(\mathbf{x}, \theta) \end{bmatrix} = \begin{bmatrix} S(x) + S\left(-\frac{x}{2} + \frac{\sqrt{3}y}{2}\right) + S\left(-\frac{x}{2} - \frac{\sqrt{3}y}{2}\right) \\ r\left(S(x + \phi(\theta)) + S_+\left(-\frac{x}{2} + \frac{\sqrt{3}y}{2}, \theta\right) + S_-\left(-\frac{x}{2} - \frac{\sqrt{3}y}{2}, \theta\right)\right) \end{bmatrix},$$

where

$$C(x) = \cos(k_c x) \quad \text{and} \quad S(x) = \sin(k_c x),$$

and

$$C_\pm(z, \theta) = C(z + \phi(\theta \mp 2\pi/3)), \quad S_\pm(z, \theta) = S(z + \phi(\theta \mp 2\pi/3)).$$

The interpretation in these cases is not as straightforward. Unlike the roll and square solutions, hexagonal and triangular solutions $A(\mathbf{x}, \theta)$ are not simply described by translated versions of $P(\mathbf{x})$. However, the locations of the maxima of $A(\mathbf{x}, \theta)$ and $P(\mathbf{x})$ do appear to be translated relative to each other. For example, the hexagonal solution for $P(\mathbf{x})$ has maximum concentration at the origin (and vertices of the hexagon). For $A(\mathbf{x}, \theta)$ it appears that the max concentration from the origin is translated to locations in the direction of $(\cos(\theta), \sin(\theta))$. In Fig. 7 we show the density plot of $P(\mathbf{x})$ along with $A(\mathbf{x}, \theta)$ for $\theta = n\pi/3$, $n = 0, ..., 5$ corresponding to particles moving along the directions of the hexagonal lattice. We observe similar behavior for the triangular solution.

6. Planforms for discrete velocities on a square lattice

6.1. Marginal stability

Following our analysis of the isotropic case, we first show that the nullspace of $L_0^S(k)$, which is defined in equation (4.15), is not contained in $V^{S,-}$. The spaces $V_S^\pm$ are defined before equation (4.13).

Proposition 6.1. *For each $k \in \mathbb{R}$, the subspace $V^{S,-}$ decomposes into the eigenspaces*

$$V^{S,-} = span\left(\begin{bmatrix} 0 \\ 1 \\ -1 \\ 0 \\ 0 \end{bmatrix}\right) \oplus span\left(\begin{bmatrix} 0 \\ 0 \\ 0 \\ 1 \\ -1 \end{bmatrix}\right)$$

with nonzero eigenvalues $-\frac{4}{3} \pm ik$.

Proof. Proof in Appendix A.4

Thus if $L_0^S(k)$ has a nullspace it must be contained in $V^{S,+}$. It turns out that the conditions for the existence of a nullspace are identical to the isotropic velocity case. Therefore, in the following proposition we reference proposition 5.3 and give the form of the nullvector.

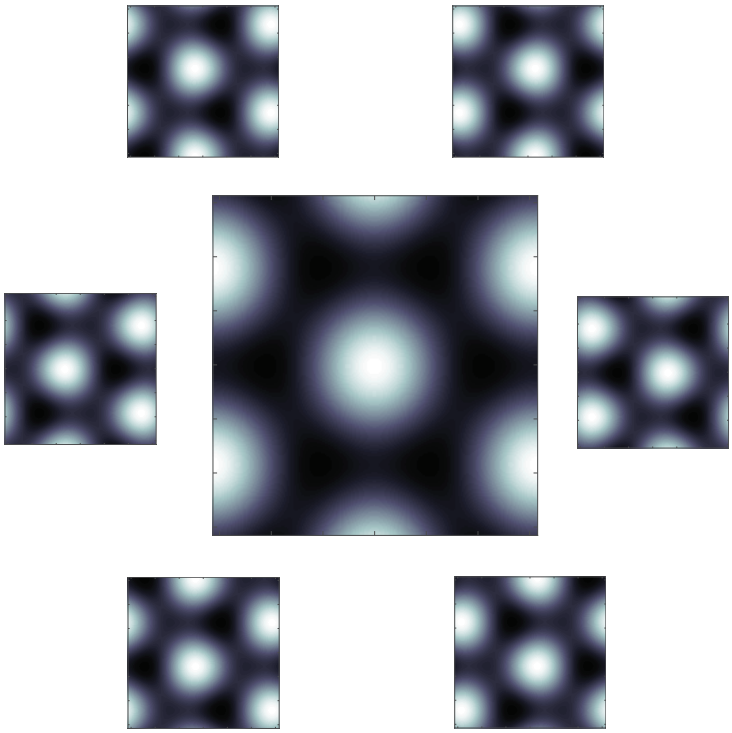

Figure 7: Same as Fig. 5 for hexagonal solutions with $\theta = n\pi/3$, $n = 0, ..., 5$ with corresponding $A(\mathbf{x}, \theta)$ in those corresponding positions.

Proposition 6.3. *Proposition 5.3 applies to the matrix $L_0^S(k)$, except that in case (b) the null vector is given by*

$$\mathbf{u} = \begin{bmatrix} 1 \\ a \\ a \\ \overline{a} \\ \overline{a} \end{bmatrix}, \quad a = \frac{2\gamma_c k_c^2 - f_p}{4f_A}\left(1 - i\frac{3k_c}{4}\right)$$

Proof. Proof in Appendix A.5.

We now show that, at $\gamma = \gamma_c$ and $k = k_c$, all other eigenvalues of $L_0(k)$ have negative real part. One of the necessary and sufficient conditions for the existence of a nullspace is that g_A and f_P are opposite in sign. It may be the case that the following result does not depend on the choice $g_A < 0$ or $g_A > 0$, but throughout the remaining analysis we will take $g_A < 0$. Not only is this mathematically convenient, but also this was the choice taken in [9].

Corollary 6.5. *Assume the conditions in propositions 4.7 and 6.3 hold. If $g_A < 0$ then, at $\gamma = \gamma_c$ and $k = k_c$, all other eigenvalues of $L_0(k)$ have negative real part.*

PROOF. Proof in Appendix A.6

In the case of discrete velocities on the square lattice, we can additionally prove that the system undergoes a Turing bifurcation.

Theorem 6.7. *Under the restrictions in propositions 4.7 and 6.3, equation (3.11) (for $N = 4$) undergoes a Turing bifurcation at $\gamma = \gamma_c$. At $\gamma = \gamma_c$ the nullspace is given by*

$$W^S \equiv null(\mathbb{L}) = \left\{ \sum_{n=1}^{2} z_n \mathbf{u}_n e^{i\mathbf{k}_n \cdot \mathbf{x}} + c.c. \;\middle|\; \forall z_n \in \mathbb{C} \right\} \cong \mathbb{C}^2$$

where

$$\mathbf{k}_1 = k_c(1,1), \quad \mathbf{k}_2 = R_{\pi/2}\mathbf{k}_1, \quad \mathbf{u}_1 = \mathbf{u}, \quad \mathbf{u}_2 = \mathbb{P}_{\pi/2}^{-1}\mathbf{u}$$

and $\mathbf{u}$ is given in proposition 6.3. For $\gamma > \gamma_c$ the uniform solution is stable, while for $\gamma < \gamma_c$ it destabilizes with the dominant growing modes given by $null(\mathbb{L})$.

PROOF. The stability results follow from proposition B.1 in the appendix. The nullspace follows from symmetry. Let the one-dimensional nullspace of $L_0^S(k)$ be spanned by $\mathbf{u}$. Then one solution to the linearized system of (3.11) is given by $\mathbf{u}e^{i\mathbf{k}_c \cdot \mathbf{x}}$. The group orbit of this solution yields other solutions

$$\mathbb{P}_{\sigma_n}^{-1}\mathbf{u}e^{i(\sigma_n \mathbf{k}_c)\cdot \mathbf{x}}$$

where we label $\sigma_n \in \mathbf{D}_4$ as

$$\sigma_1 = I, \quad \sigma_2 = R_{\pi/2}, \quad \sigma_3 = \kappa, \quad \sigma_4 = \kappa R_{\pi/2}, \quad \sigma_{4+j} = -\sigma_j \quad j = 1, 4.$$

Recall that if $\{\mathbf{u}, \lambda\}$ is an eigenpair for $L(\mathbf{k})$ then $\{\overline{\mathbf{u}}, \overline{\lambda}\}$ is an eigenpair for $L(-\mathbf{k})$. Therefore, since $\lambda = 0$ at the critical wavevector,

$$\sigma_{4+j}\mathbf{k}_c = -\sigma_j \mathbf{k}_c \implies \mathbb{P}_{\sigma_{4+j}}^{-1}\mathbf{u} = \mathbb{P}_{\sigma_j}^{-1}\overline{\mathbf{u}},$$

and the nullspace can be represented by

$$\left\{ \sum_{n=1}^{4} z_n \mathbb{P}_{\sigma_n}^{-1}\mathbf{u}e^{i(\sigma_n \mathbf{k}_c)\cdot \mathbf{x}} + c.c \;\middle|\; \forall z_n \in \mathbb{C} \right\}. \tag{6.1}$$

In general, in contrast to solutions to $\mathbf{E}(2)$-equivariant systems, we have $N = 4$ linearly independent terms instead of 2. For $\mathbf{E}(2)$-equivariant systems one can set $\kappa\mathbf{k}_c = \mathbf{k}_c$ by taking a rotation, and thus the $n = 3, 4$ terms are redundant. However such a rotation does not exist in $\mathbf{D}_4$ unless $\mathbf{k}_c$ happens to lie on an axis of reflection in $\mathbf{D}_4$. In our case we have that $\mathbf{k}_c = k_c(\boldsymbol{\ell}_1 + \boldsymbol{\ell}_2)$ which points along the diagonal of the square lattice and thus

$$\kappa\mathbf{k}_c = -R_{\pi/2}\mathbf{k}_c.$$

Therefore, the number of linearly independent terms reduces to 2 and we have the standard 4 dimensional representation.

6.2. Planforms on a square lattice

In the following calculations, we make use of the fact that, according to theorem 6.7, square solutions have the form

$$\begin{bmatrix} p(\mathbf{x}) \\ a_0(\mathbf{x}) \\ a_1(\mathbf{x}) \\ a_2(\mathbf{x}) \\ a_3(\mathbf{x}) \end{bmatrix} = z_1 \begin{bmatrix} 1 \\ a \\ a \\ \overline{a} \\ \overline{a} \end{bmatrix} e^{ik_c(x+y)} + z_2 \begin{bmatrix} 1 \\ \overline{a} \\ a \\ a \\ \overline{a} \end{bmatrix} e^{ik_c(-x+y)} + c.c.$$

since $\mathbb{P}_{\pi/2}^{-1}$ cyclically shifts the second through fifth components down by one. We then set values of z_n depending on the isotropy subgroup according to proposition 5.7. Again, looking at the total concentration of AT particles

$$\mathcal{A}(\mathbf{x}) = \sum_{n=0}^{3} a_n(\mathbf{x}) = 2\mathrm{Re}(a)p(\mathbf{x}) = \frac{2\gamma_c k_c^2 - f_P}{2f_A} p(\mathbf{x})$$

we see that it is a constant multiple of the concentration of PT particles. Now

$$2\gamma_c k_c^2 - f_P = \frac{16}{3}\gamma_c g_A - \frac{1}{2} f_P < 0$$

since $g_A < 0$ and $f_P > 0$. Thus, as in the isotropic case, $\mathcal{A}$ and P are in phase if $f_A < 0$ and antiphase if $f_A > 0$.

We now analyze the individual components $a_i(\mathbf{x})$. Similar to the isotropic case, we set

$$\phi = -\frac{1}{k_c}\arg(a) = -\frac{1}{k_c}\arg\left(1 - i\frac{3k_c}{4}\right),$$

where a is defined in proposition 6.3. Note that we use "-" so that $\phi > 0$. Then, near bifurcation, solutions have the following forms up to a real constant multiple.

1. Rolls: In this case we can set $(z_1, z_2) = (1, 0)$. Then defining

   $$R(x, y) = \cos(k_c(x + y))$$

   we have

   $$\begin{bmatrix} p(\mathbf{x}) \\ a_0(\mathbf{x}) \\ a_1(\mathbf{x}) \\ a_2(\mathbf{x}) \\ a_3(\mathbf{x}) \end{bmatrix} = \begin{bmatrix} R(x, y) \\ |a|R(x - \phi, y) \\ |a|R(x, y - \phi) \\ |a|R(x + \phi, y) \\ |a|R(x, y + \phi) \end{bmatrix}$$

   In contrast to the isotropic case, we must define the roll pattern with wave vector $\mathbf{k} = k_c(1, 1)$ instead of the standard $\mathbf{k} = k_c(1, 0)$. This is due to the fact that we found the critical wavevector to have the former form, and the latter form is not on the same orbit with respect to the group action of $\mathbf{D}_4$.

2. Squares: In this case we can set $(z_1, z_2) = (1, 1)$. Then defining

$$S(x, y) = \cos(k_c(x + y)) + \cos(k_c(-x + y))$$

we have

$$\begin{bmatrix} p(\mathbf{x}) \\ a_0(\mathbf{x}) \\ a_1(\mathbf{x}) \\ a_2(\mathbf{x}) \\ a_3(\mathbf{x}) \end{bmatrix} = \begin{bmatrix} S(x, y) \\ |a|S(x - \phi, y) \\ |a|S(x, y - \phi) \\ |a|S(x + \phi, y) \\ |a|S(x, y + \phi) \end{bmatrix}$$

Again, the square solution in this case is distinct from that in the isotropic case due to the particular direction of the critical wavevector.

Both solution types have the same interpretation as in the isotropic case. The PT concentration $p(\mathbf{x})$ has its maximum at the origin, modulo the lattice. The functions $a_0(\mathbf{x})$ and $a_2(\mathbf{x})$ denote the concentrations of AT particles with velocities in the positive and negative x-directions respectively, while $a_1(\mathbf{x})$ and $a_4(\mathbf{x})$ correspond to velocities in the positive and negative y-directions, respectively. Since the functions $a_i(\mathbf{x})$ are simply translated versions of $p(\mathbf{x})$, we see that the concentrations of AT particles with horizontal velocity have maxima at $(x, y) = (\pm\phi, 0)$ while those with vertical velocities have maximums at $(x, y) = (0, \pm\phi)$. This is consistent with what we saw for the isotropic case when choosing $\theta = 0, \pi/2, 3\pi/2$, which directly correspond to $a_0, ..., a_3$. The only difference is the orientation of the pattern. That is, the pattern for $p(\mathbf{x})$ in the discrete velocity case is a rotated version of the $p(\mathbf{x})$ in the isotropic case.

7. Discussion

In this paper, we used symmetric bifurcation theory to analyze the emergence of Turing patterns in a two dimensional hybrid reaction-transport model. We assumed that the active particles were transported either (i) isotropically at a constant speed v or (ii) via a discrete set of velocities (still with constant speed) in directions along a lattice tiling the plane. In the former case the system was equivariant with respect to the shift-twist action of the Euclidean group $\mathbf{E}(2)$ acting on functions on $\mathbb{R}^2 \times \mathbf{S}^1$, while in the latter case it was equivariant with respect to the group $\mathbf{D}_N \ltimes \mathbb{R}^2$ where $\mathbf{D}_N$ ($N = 4$ for square and $N = 6$ for hexagonal) is the holohedry group of the lattice. In the discrete velocity square lattice case, we derived necessary and sufficient conditions for a Turing bifurcation to occur as the dimensionless parameter $\gamma = \alpha D/v^2$ crosses some critical value; in the other cases we were only able to derive necessary conditions. However, in all cases we could determine the associated bifurcating planforms. In particular, we found that the periodically varying AT concentration was a shifted version of the PT concentration pattern, with the transformation depending on the velocity direction.

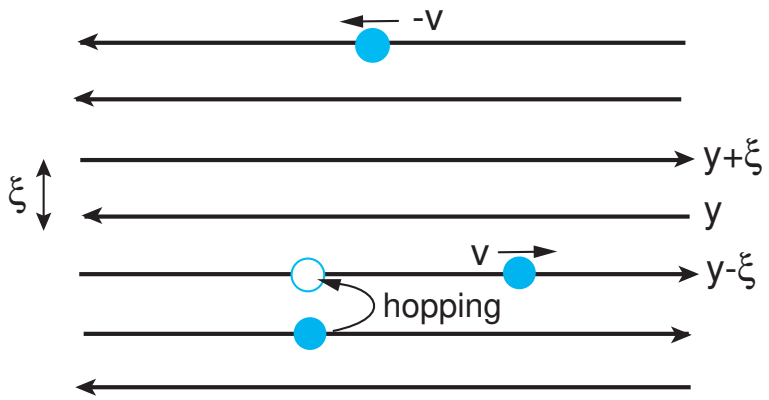

Figure 8: Random velocity model of a microtubular network with quenched polarity disorder. Active particles move ballistically along parallel tracks in a direction determined by the polarity of the given track. They also hop between tracks according to an unbiased random walk.

The main simplification of our model was to treat the microtubular network as a homogeneous domain, in the sense that at any point the active particles have access to the same set of velocity directions. As noted in the introduction, a more detailed microscopic model of intracellular transport within the cell would need to specify the spatial distribution of microtubular orientations and polarity, in order to determine which velocity states are available to a motor-cargo complex at a particular spatial location. This suggests considering alternative models, in which the discrete nature of microtubular networks is taken into account. One possibility would be to adapt an alternative formulation of transport on disordered microtubular networks, based on random velocity fields [26, 22, 19]. In order to illustrate this type of model, consider a set of equally spaced parallel tracks along the x-axis, say, see Fig. 8. The tracks are assigned random polarities ± 1 with equal probabilities corresponding to quenched polarity disorder. An active particle undergoes a random walk in the y–direction, whereas when a particle attaches to a certain track it moves ballistically with velocity ± 1 according to the track's polarity. It is assumed that when a particle hops to a neighboring track it binds immediately.

One of the interesting features of the random velocity model is that it exhibits anomalous diffusion. Let $X(t)$ denote the displacement of a random walker in the longitudinal direction at time t:

$$X(t) = \int_0^t v[y(t')]dt'. \tag{7.1}$$

Taking the continuum limit in the y direction means that

$$p(y,t) = \frac{1}{\sqrt{4\pi Dt}} \mathrm{e}^{-y^2/4Dt},$$

where D is the diffusion coefficient, and the velocity field is δ–correlated,

$$\langle v(y)v(y')\rangle_c = v^2\xi\delta(y-y').$$

Here averaging is taken with respect to the quenched polarity disorder and ξ is the infinitesimal spacing between tracks. Now consider the second moment $\langle\langle X^2(t)\rangle\rangle$ of the stochastic process averaged with respect to the quenched disorder and realizations of the random walk:

$$\langle\langle X^2(t)\rangle\rangle = 2\int_0^t dt_1 \int_0^{t_1} dt_2 \langle\langle v[y(t_1)]v[y(t_2)]\rangle\rangle, \tag{7.2}$$

where

$$\begin{aligned}\langle\langle v[y(t_1)]v[y(t_2)]\rangle\rangle = &\int_{-\infty}^{\infty} dy_1 \int_{-\infty}^{\infty} dy_2 \langle v(y_1)v(y_2)\rangle_c \\ &\times p(y_2,t_2)p(y_1-y_2,t_1-t_2).\end{aligned} \tag{7.3}$$

Using Laplace transforms and the velocity correlation function,

$$\langle\langle \widetilde{X}^2(s)\rangle\rangle = \frac{2v^2\xi}{s}\widetilde{p}(0,s)\int_{-\infty}^{\infty}\widetilde{p}(y,s)dy, \tag{7.4}$$

with

$$\widetilde{p}(y,s) = \frac{1}{\sqrt{4Ds}}\mathrm{e}^{-|y|\sqrt{s/D}}.$$

Performing the integration with respect to y thus shows that $\langle\langle \widetilde{X^2}(s)\rangle\rangle = v^2\xi D^{-1/2}s^{-5/2}$, which on inverting the Laplace transform gives

$$\langle\langle X^2(t)\rangle\rangle = \frac{4v^2\xi}{3\sqrt{\pi D}}t^{3/2}. \tag{7.5}$$

This establishes that the random velocity model supports anomalous superdiffusion in the x direction. Within the context of the current paper, it would be interesting to extend the above model by including a second chemical species, which diffuses in the plane and reacts with the active particles. Again, any symmetries of the underlying network configuration will impact the type of patterns that can emerge.

One final comment is in order. As far as we are aware, higher-dimensional analogs of synaptogenesis in *C. elegans* have not yet been observed. Nevertheless, the latter example suggests that hybrid reaction-transport processes could provided an alternative Turing mechanism to classical reaction-diffusion systems in cells, some of the consequences of which we have explored in this paper.

Appendix A. Proofs

Appendix A.1. Proof of proposition 4.7

Setting $\mathbf{k} = 0$ in equation (4.3) for the isotropic case, yields

$$\lambda p = f_P p + f_A \int_0^{2\pi} a(\theta) d\theta \tag{A.1}$$

$$\lambda a(\theta) = g_P p - a(\theta) + \left(\frac{1}{2\pi} + g_A\right) \int_0^{2\pi} a(\theta) d\theta, \tag{A.2}$$

while setting $\mathbf{k} = 0$ in equation (4.10) for the discrete case gives

$$\lambda p = f_p p + f_A \sum_{n=1}^{N} a_n \tag{A.3a}$$

$$\lambda a_j = g_p p + (g_A - 1) a_j + \left(\frac{1}{N-1} + g_A\right) \sum_{n \neq j} a_n, \quad j = 0, \ldots, N-1. \tag{A.3b}$$

In both cases, we show that there are two different types of eigenfunctions: (i) $\int a(\theta) = 0$ for isotropic velocities and $\sum_j a_j = 0$ for discrete velocities, and (ii) $a(\theta)$ and a_j are constants.

In the case of type (i) eigenfunctions, we have

$$\lambda p = f_P p$$
$$\lambda a(\theta) = g_P p - a(\theta)$$

for isotropic velocities and

$$\lambda p = f_p p$$
$$\lambda a_j = g_p p - \frac{N}{N-1} a_j$$

for discrete velocities. If $p \neq 0$, then the second equation for isotropic (discrete) velocities is satisfied only if $a(\theta)$ (a_j) is a non-zero constant, which violates $\int a(\theta) = 0$ ($\sum a_j = 0$). Thus there are no solutions with $p \neq 0$. Therefore, taking $p = 0$ we find the following eigenvalues and eigenfunctions:

$$\lambda = -1, \quad (p, a(\theta)) = (0, e^{in\theta}) \text{ for all integers } n > 0,$$

in the isotropic case, and

$$\lambda = -\frac{N}{N-1}, \quad \begin{bmatrix} p \\ \mathbf{a} \end{bmatrix} = \mathbf{e}_2 - \mathbf{e}_3, \quad \ldots \quad \mathbf{e}_N - \mathbf{e}_{N+1}$$

in the discrete case, where $\mathbf{e}_i$ are the standard basis vectors for $\mathbb{R}^{N+1}$.

Now consider type (ii) eigenfunctions for which $\int a(\theta) \neq 0$ ($\sum a_j \neq 0$), in which case $a(\theta) = \bar{a}$ ($a_j = \bar{a}$) with $\bar{a}$ a constant. This yields a standard 2×2 eigenvalue problem

$$\lambda p = f_P p + \Omega f_A \bar{a}$$
$$\lambda \bar{a} = g_P p + \Omega g_A \bar{a}$$

where $\Omega = 2\pi$ for the isotropic case and $\Omega = N$ for the discrete case. It is a standard result that both eigenvalues of a 2×2 matrix have negative real parts if and only if the trace is negative and the determinant is positive. The trace and determinant of the coefficient matrix are given by

$$\beta_\Omega = f_P + \Omega g_A \quad \text{and} \quad \Omega\delta = \Omega(f_P g_A - f_A g_P)$$

respectively, thus proving the claim since $\Omega > 0$.

Appendix A.2. Dispersion relation: Proof of proposition 5.1

First, we solve equation (4.4b) for $a(\theta)$ to obtain

$$a(\theta) = \left[\left(\frac{1}{2\pi} + g_A\right)\int a(\theta)d\theta + g_P p\right]\frac{1}{ik\cos(\theta) + 1 + \lambda}.$$

Integrating with respect to θ and solving for the integral yields

$$\int a(\theta)d\theta = \frac{2\pi g_P p h(\lambda, k)}{1 - (1 + 2\pi g_A)h(\lambda, k)}$$

where we defined

$$h(\lambda, k) = \frac{1}{2\pi}\int_0^{2\pi} \frac{1}{ik\cos(\theta) + 1 + \lambda} d\theta = -\frac{1}{\pi k}\oint_{|z|=1} \frac{1}{z^2 - 2\frac{1+\lambda}{k} iz + 1} dz.$$

We obtain the second equality by complexifying the integral, letting $z = e^{i\theta}$ and writing $\cos(\theta) = (z + 1/z)/2$. We note that if $\lambda + 1 = i\omega$ for $\omega \in \mathbb{R}$ and $|\omega| \leq k$, then the integral does not converge.

Imposing consistency, we solve for $\int a$ in equation (4.4a) and equate it with the above expression to yield the dispersion relation

$$\frac{2\pi g_P f_A h(\lambda, k)}{1 - (1 + 2\pi g_A)h(\lambda, k)} = \lambda + \gamma k^2 - f_P. \tag{A.4}$$

We assume $p \neq 0$ when simplifying the equation. This assumption is justified because if $p = 0$, then equation (4.3a) implies $\int a = 0$ and thus (4.3b) implies

$$\lambda a(\theta) = -[ik\cos(\theta) + 1]a(\theta)$$

which, for $k \neq 0$, only holds when $a(\theta) = 0$ (the $k = 0$ case was already considered in Section 3.2.1). Thus there are no eigenvectors with $p = 0$ and $a(\theta) \neq 0$. Moreover, if $h(\lambda, k) = 1 + 2\pi g_A$ for some (λ, k) then $p = 0$ necessarily

by the first expression in this proof. Therefore, it must be that $a(\theta) = 0$ and the corresponding λ is not an eigenvalue.

Now $h(\lambda, k)$ can be computed using the residue theorem for complex contour integrals for $k \neq 0$. If $k = 0$ then the integral is

$$h(\lambda, 0) = \frac{1}{1+\lambda}.$$

Otherwise, the singularities of the integrand are

$$r_{\pm}(\lambda, k) = \frac{i}{k}\left[1 + \lambda \pm ((1+\lambda)^2 + k^2)^{1/2}\right].$$

For notational simplicity let $\omega = (1+\lambda)/k$ so that the singularities can be written as

$$r_{\pm}(\omega) = i\left[\omega \pm (\omega^2 + 1)^{1/2}\right]$$

where we define $(\omega^2+1)^{1/2}$ in the usual way with branch cut on $(-i\infty, -i] \cup [i, i\infty)$ so that it is continuous on the real line.

Note that $|r_+|$ and $|r_-|$ cannot both be less than one nor both greater than one. This can be seen by taking the product

$$r_+ r_- = 1$$

and thus $|r_+||r_-| = 1$. Therefore, using the residue theorem

$$\begin{aligned}
\oint_{|z|=1} \frac{1}{z^2 - 2i\omega z + 1} &= 2\pi i \begin{cases} \text{Res}(I, r_+(\omega)), & |r_+(\omega)| < 1 \\ \text{Res}(I, r_-(\omega)), & |r_-(\omega)| < 1 \end{cases} \\
&= 2\pi i \begin{cases} \text{Res}(I, r_+(\omega)), & |r_+(\omega)| < 1 \\ \text{Res}(I, r_-(\omega)), & |r_+(\omega)| > 1 \end{cases} \\
&= \pi \begin{cases} (\omega^2+1)^{1/2}, & |r_+(\omega)| < 1 \\ -(\omega^2+1)^{1/2}, & |r_+(\omega)| > 1 \end{cases}
\end{aligned}$$

where I is the integrand. Therefore

$$h(\omega, k) = \frac{1}{k} \begin{cases} (\omega^2+1)^{-1/2}, & |r_+(\omega)| > 1 \\ -(\omega^2+1)^{-1/2}, & |r_+(\omega)| < 1 \end{cases}.$$

It is straightforward to show that $|r_+(\omega)| < 1$ if $\text{Re}(\omega) < 0$ and $|r_+(\omega)| > 1$ if $\text{Re}(\omega) > 0$ and we can equivalently define

$$h(\omega, k) = \frac{1}{k}(\omega^2+1)^{-1/2}$$

taking the branch cut as the straight line between $-ik$ and ik and letting $h(\omega, k) > 0$ for real values of $\omega > 0$ and $h(\omega, k) < 0$ for real values of $\omega < 0$.

Rewriting in terms of λ, multiplying (A.4) by $((\lambda+1)^2 + k^2)^{1/2}$ and rearranging terms yields the result. The form of the eigenvector is clear by rewriting the expression for $a(\theta)$ in the first equation in this proof and using the equality in (A.4).

Appendix A.3. Proof of proposition 5.3

First we rewrite equation (5.2) as

$$\frac{\gamma}{f_P} = \frac{w - w_1}{((w+1)^2 - 1)(w - w_2)} \tag{A.5}$$

where we have set

$$w = \sqrt{1+k^2} - 1, \quad w_1 = \frac{2\pi\delta}{f_P}, \quad \text{and} \quad w_2 = 2\pi g_A.$$

Note that $w \geq 0$ and has a monotonic dependence on $k \geq 0$. By proposition 4.7, we have that $\delta = f_P g_A - f_A g_P > 0$ and $f_P + 2\pi g_A < 0$. The former implies that w_1 and f_P have the same sign and the latter implies that w_1 and w_2 cannot both be positive. Moreover, there are no solutions when w_1 and w_2 are both negative. Hence we require that $w_1 w_2 < 0$.

We proceed with a graphical construction of the critical values k_c and γ_c. In Figure A.9 we show qualitative graphs of the right hand side of equation (A.5) (for both cases of $w_1 w_2 < 0$) along with the line $2\gamma/f_P$ for different values of γ. In both cases it is clear that there exists a γ_c such that, at $\gamma = \gamma_c$, there is only one solution. In the case $w_2 < 0 < w_1$, for $\gamma < \gamma_c$ there are two solutions and for $\gamma > \gamma_c$ there are no solutions. In the case $w_1 < 0 < w_2$ the inequalities for γ are reversed. Since w is monotonic in $k \geq 0$, then the same solution structure applies to k.

Finally, the form of $a(\theta)$ follows from proposition 5.1.

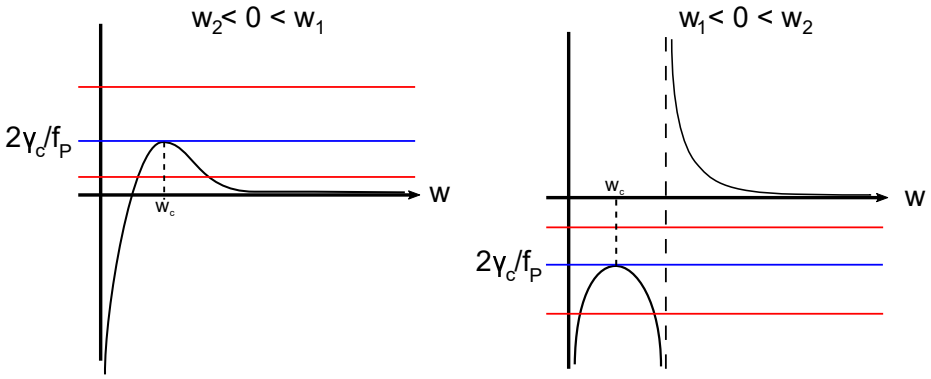

Figure A.9: Qualitative graphs of equation A.5. Black lines are graphs of the right hand side, while colored lines are the left hand side. Blue lines indicate parameter values for which there exist a single solution and red lines indicate no or two solutions.

Appendix A.4. Proof of proposition 6.1

Substituting $\mathbf{u} \in V^{S,-}$ into equation (4.13) yields the reduced system

$$\begin{aligned}
\lambda p &= (-2\gamma k^2 + f_p)p \\
\lambda a &= -\left(ik + \frac{4}{3}\right) a + g_P p \\
\lambda b &= -\left(-ik + \frac{4}{3}\right) b + g_P p
\end{aligned}$$

The 3×3 system is lower triangular and thus has eigenvalues

$$\lambda = -2\gamma k^2 + f_p, \quad -\frac{4}{3} \pm ik,$$

with corresponding eigenvectors

$$\begin{bmatrix} p \\ a \\ b \end{bmatrix} = \begin{bmatrix} \frac{1}{3g_P} \\ \frac{1}{4+3f_P-6\gamma k^2+3ik} \\ \frac{1}{4+3f_P-6\gamma k^2-3ik} \end{bmatrix}, \begin{bmatrix} 0 \\ 1 \\ 0 \end{bmatrix}, \begin{bmatrix} 0 \\ 0 \\ 1 \end{bmatrix}$$

Since the first eigenvector of the reduced system has $p \neq 0$, it cannot possibly correspond to a vector in $V^{S,-}$. The second two reduced eigenvectors correspond to the vectors, in the full 5×5 system,

$$\begin{bmatrix} 1 \\ -1 \\ 0 \\ 0 \end{bmatrix}, \quad \begin{bmatrix} 0 \\ 0 \\ 1 \\ -1 \end{bmatrix}$$

with eigenvalues $-\frac{4}{3} \pm ik$.

Appendix A.5. Proof of proposition 6.3

Substituting $\mathbf{u} \in V^{S,+}$ into (4.13) yields the reduced system

$$\begin{aligned}
\lambda p &= (-2\gamma k^2 + f_P)p + 2f_A(a+b) \\
\lambda a &= -\left(ik + \frac{2}{3} - 2g_A\right) a + \left(\frac{2}{3} + 2g_A\right) b + g_P p \\
\lambda b &= -\left(-ik + \frac{2}{3} - 2g_A\right) b + \left(\frac{2}{3} + 2g_A\right) a + g_P p.
\end{aligned}$$

The determinant of the matrix is given by

$$\frac{1}{3}\left(-6\gamma k^4 + (32\gamma g_A + 3f_P)k^2 - 16\delta\right).$$

Setting it equal to zero and rearranging terms yields

$$\frac{2\gamma}{f_P} = \frac{k^2 - k_1}{k^2(k^2 - k_2)} \tag{A.6}$$

where $k_1 = \frac{16\delta}{3f_P}$ and $k_2 = \frac{16g_A}{3}$. By proposition 4.7 $\delta = f_P g_A - f_A g_P > 0$ and $\beta_N = f_p + N g_A < 0$. The former implies that k_1 has the same sign as f_P and the latter implies that k_1 and k_2 cannot both be positive. Moreover, k_1 and k_2 cannot both be negative. If they were, the right hand side of equation (A.6) would be positive for all k, while the left hand side is negative. Thus there would be no solutions. Hence a necessary condition for the existence of a solution is that $k_1 k_2 < 0$ and consequently $f_P g_A < 0$. This together with $\delta > 0$ implies that $f_A g_P < 0$. The graph of the right hand side of equation (A.6) is qualitatively identical to the graph of the right hand side of equation (A.5) and the left hand sides only differ by a factor of 2. Thus the remainder of the proof is identical to the proof for proposition 5.3.

Since the nullspace is one-dimensional, Corollary 4.5 along with the fact that $\mathbf{u} \in V^{S,+}$ implies that null-vectors have the form

$$\mathbf{u} = \begin{bmatrix} p \\ a \\ a \\ \overline{a} \\ \overline{a} \end{bmatrix}.$$

Substituting $\mathbf{u}$ into the reduced system, setting $\lambda = 0$ and $p = 1$, and solving for a gives the expression for the null vector.

Appendix A.6. Proof of corollary 6.5

At $k = k_c, \gamma = \gamma_c$ the characteristic polynomial of L_0^S restricted to $V^{S,+}$ is factored as

$$-\frac{1}{3}\lambda\left[3\lambda^2 + (6\gamma_c k_c^2 - 3\beta + 4)\lambda + (3 + 8\gamma_c - 24\gamma_c g_A)k_c^2 + 12\delta - 4\beta\right].$$

Thus the remaining eigenvalues are

$$\frac{1}{6}\left(-(6\gamma_c k_c^2 - 3\beta + 4) \pm \sqrt{(6\gamma_c k_c^2 - 3\beta + 4)^2 - 12(3 + 8\gamma_c - 24\gamma_c g_A)k^2 - 36\delta + 48\beta}\right) \tag{A.7}$$

The conditions $\beta < 0$, $\delta > 0$ established in proposition 4.7, along with the assumption that $g_A < 0$ and $\gamma_c > 0$, guarantee that the above expression has negative real part. If these eigenvalues are complex-valued, then the real part is

$$-\frac{1}{6}(6\gamma_c k_c^2 - 3\beta + 4) < 0.$$

Otherwise, if they are real, the square root term is bounded by

$$|6\gamma_c k_c^2 - 3\beta + 4|$$

and so it is clear that both eigenvalues are negative. This shows that the nullspace of the full matrix $L_0^S(k)$ must be one-dimensional at $k = k_c$ and only has 5 eigenvalues counting multiplicity. Proposition 6.1 shows that there are 2 eigenvalues corresponding to the subspace $V^{S,-}$ and here we have found the remaining 3 eigenvalues, two of which have negative real part.

Appendix B. Bifurcation analysis for square discrete velocities

We now derive conditions for the existence of a Turing bifurcation from the homogeneous fixed point to doubly periodic solutions for the discrete velocity model on a square lattice. We use the dimensionless parameter γ as the bifurcation parameter and look for a critical value γ_c such that when $\gamma = \gamma_c$ the $L(\mathbf{k})$ has a one dimensional nullspaces at some critical wavevector $\mathbf{k}_c$ (and by symmetry all orbits $\sigma\mathbf{k}_c$, $\sigma \in \mathbf{O}(2)$ (or $\mathbf{D}_N$). We must determine conditions under which the following hold:

(a) $\mathrm{Re}[\lambda(0)] < 0$ for all γ in some neighborhood of γ_c

(b) For $\gamma < \gamma_c$ (or $\gamma > \gamma_c$ depending on the direction of bifurcation) sufficiently close, $\mathrm{Re}(\lambda(\mathbf{k})) < 0$ for all eigenvalues λ and $\mathbf{k} \in \mathbb{R}^2$

(c) For $\gamma = \gamma_c$, at $\mathbf{k} = \mathbf{k}_c$ there exists a zero eigenvalue with multiplicity 1 and all other eigenvalues $\mathrm{Re}(\lambda(\mathbf{k}_c)) < 0$. For $\mathbf{k} \neq \mathbf{k}_c$ all eigenvalues satisfy $\mathrm{Re}(\lambda(\mathbf{k})) < 0$.

(d) For $\gamma > \gamma_c$ (or $\gamma < \gamma_c$) sufficiently close, there exists a neighborhood $\mathcal{N}(\mathbf{k}_c)$ of $\mathbf{k}_c$ such that (i) for each $\mathbf{k} \in \mathcal{N}(\mathbf{k}_c)$ there is one eigenvalue with $\mathrm{Re}(\lambda(\mathbf{k})) > 0$) and all other eigenvalues have $\mathrm{Re}(\lambda(\mathbf{k}) < 0)$ and (ii) for each $\mathbf{k} \notin \mathcal{N}(\mathbf{k}_c)$ all eigenvalues satisfy $\mathrm{Re}(\lambda(\mathbf{k})) < 0$.

We have already shown (a) and (c) and thus only need to establish (b) and (d).

Proposition B.1 *Assume all the conditions in propositions 4.7 and 6.3 hold, and take $g_A < 0, f_P > 0$. We then have the following:*

1. *Consider $\gamma > \gamma_c$ sufficiently close. Then for all $k \in \mathbb{R}$, all eigenvalues of $L_0(k)$ have negative real part.*
2. *Consider $\gamma < \gamma_c$ sufficiently close. Then for each $k \in N(k_c)$ (some neighborhood of k_c), $L_0(k)$ has a single positive real eigenvalue, with all others having negative real part. For each $k \notin N(k_c)$ all eigenvalues have negative real part.*

Proof. We first show that at $\gamma = \gamma_c$, all eigenvalues have negative real part. First, by proposition 6.1 the eigenvalues from the subspace V^- always have negative real part and therefore we need only consider eigenvalues from V^+. For any k and γ, the characteristic polynomial of $L_0(k)$ restricted to V^+ is

$$d(\lambda, k, \gamma) = -\lambda^3 + \left(\beta - 2\gamma k^2 - \frac{4}{3}\right)\lambda^2 + \frac{1}{3}\left(24\gamma g_A k^2 + 4\beta - 12\delta - 3k^2 - 8\gamma k^2\right)\lambda + q(k, \gamma)$$

where

$$q(k, \gamma) = \frac{1}{3}\left(-6\gamma k^4 + (32\gamma g_A + 3f_P)k^2 - 16\delta\right)$$

is the determinant. Throughout, we will make use of the fact that the non-zero degree coefficients are all negative for all γ, k since $\gamma, \delta > 0$ and $\beta, g_A < 0$. Moreover, $q(k, \gamma_c) \leq 0$ for all k with equality if and only if $k = k_c$. Finally note that proposition 6.3 showed that all roots of $d(\lambda, k_c, \gamma_c)$ have negative real part.

For $\gamma = \gamma_c$ and all $k \neq k_c$, the coefficients of $d(\lambda, k, \gamma_c)$ are all negative. Therefore, by Descarte's rule of signs there are no positive real roots. Applying the rule to $d(-\lambda, k, \gamma_c)$ implies that there are either 3 or 1 negative real roots. If there are 3 then we have completed the proof. Otherwise, there is a conjugate pair of complex roots. Since at $k = k_c$ all roots have negative real part, we must show that the roots cannot cross the imaginary axis as k increases/decreases from k_c. Thus, set $\lambda = i\omega$, $0 \neq \omega \in \mathbb{R}$. Setting the real and imaginary parts of $d(i\omega, k, \gamma_c)$ to zero yields

$$\omega^2 + \frac{1}{3}(24\gamma g_A k^2 + 4\beta - 12\delta - 3k^2 - 8\gamma k^2) = 0 \quad q(k, \gamma_c) - \left(\beta - 2\gamma k^2 - \frac{4}{3}\right)\omega^2 = 0$$

which implies that

$$q(k, \gamma_c) = -\frac{1}{3}(24\gamma_c g_A k^2 + 4\beta - 12\delta - 3k^2 - 8\gamma_c k^2)\left(\beta - 2\gamma_c k^2 - \frac{4}{3}\right).$$

We now compare the coefficients on both sides of the equation. The constant coefficient on the right hand side is

$$\frac{1}{3}(-4\beta^2 + \frac{16}{3}\beta + 12\delta\beta - 16\delta) < -\frac{16}{3}\delta$$

since $\beta < 0, \delta > 0$. Note that the upper bound is the constant coefficient for $q(k, \gamma_c)$. The k^2 coefficient for the right hand side is

$$-\left[(24\gamma_c g_A - 3 - 8\gamma)\left(\beta - \frac{4}{3}\right) - 2\gamma_c(4\beta - 12\delta)\right] < 0$$

since $g_A < 0$, while the k^2 coefficient for q is

$$\frac{1}{3}(32\gamma g_A + 3f_P) > 0$$

by the conditions in proposition 6.3. Finally, the k^4 coefficient for the right hand side is

$$\frac{2}{3}\gamma_c(24\gamma_c g_A - 3 - 8\gamma_c) < -2\gamma_c$$

with the upper bound being the k^4 coefficient for q. Since there are only even powers of k, these inequalities imply that $q(k, \gamma_c)$ is greater than the right hand side for all k. Thus, the roots of d cannot cross the imaginary axis, and thus their real parts remain negative for all k.

Now consider $\gamma < \gamma_c$ sufficiently close. Then, by construction, $q(k, \gamma) \geq 0$ for $k \in N(k_c)$ and negative elsewhere. In this case, for all $k \in N(k_c)$ the coefficients of $d(\lambda, k, \gamma)$ change once, and by Descarte's rule of signs, there is exactly one

positive real eigenvalue for each fixed k. This positive eigenvalue arises from the zero eigenvalue as γ crosses γ_c. All other roots must have negative real part by continuiity of roots of the polynomial with respect to parameter changes.

Finally consider $\gamma > \gamma_c$ sufficiently close. In this case $q(k, \gamma) < 0$ for all $k \in \mathbb{R}$. Again, by Descarte's rule of signs, there are no positive real roots and either 3 or 1 negative real roots. Using the same argument as the $\gamma = \gamma_c$ case shows that all roots must have negative real part, with one real negative roots coming from the zero eigenvalue as γ crosses γ_c.

Acknowledgments

P.C.B. and S.R.C. were supported by the National Science Foundation (Grant No. DMS-1613048).

References

[1] O. Benichou, C. Loverdo, M. Moreau and R. Voituriez. A minimal model of intermittent search in dimension two. J. Phys. A 19 (2007) 065141.

[2] I. Bosch Vivancos, P. Chossat and I. Melbourne. New planforms in systems of partial differential equations with Euclidean symmetry. Arch. Rat. Mech. Anal. 131 (1995) 199–224.

[3] P. C. Bressloff, J. D. Cowan, M. Golubitsky, P. J. Thomas and M. Wiener. Geometric visual hallucinations, Euclidean symmetry and the functional architecture of striate cortex. Phil. Trans. Roy. Soc. B 40 (2001) 299-330.

[4] P. C. Bressloff, J. D. Cowan, M. Golubitsky and P. J. Thomas. Scalar and pseudoscalar bifurcations motivated by pattern formation on the visual cortex. Nonlinearity 14 (2001) 739-775.

[5] P. C. Bressloff. Euclidean shift-twist symmetry in population models of self-aligning objects. SIAM J. Appl. Math. 64 (2004) 1668-1690.

[6] P. C. Bressloff and J. M. Newby. Quasi-steady state analysis of motor-driven transport on a two-dimensional microtubular network. Phys. Rev. E. 83 (2011) 061139.

[7] P. C. Bressloff and J. M. Newby. Stochastic models of intracellular transport. Rev. Mod. Phys. 85 (2013) 135-196.

[8] P. C. Bressloff. Stochastic Processes in Cell Biology. Springer (2014).

[9] H. A. Brooks and P. C. Bressloff. A mechanism for Turing pattern formation with active and passive transport. SIAM J. Appl. Dyn. Syst. 15 (2016) 1823-1843

[10] H. A. Brooks and P. C. Bressloff. Turing mechanism for homeostatic control of synaptic density in C. elegans. Phys. Rev. E. 96 (2017) 012413.

[11] E. M. Damm and L. Pelkmans. Systems biology of virus entry in mammalian cells. Cell Microbiol. 8, (2006) 1219-1227.

[12] A. Gierer and H. Meinhardt., A theory of biological pattern formation, Kybernetik, 12 (1972) 30–39.

[13] M. Golubitsky and I. Stewart. The symmetry perspective: from equilibrium to chaos in phase space and physical space, Birkhauser, Basel (2002).

[14] M. Golubitsky, I. Stewart, and D.G. Shaeffer. Singularities and groups in bifurcation theory II, Springer-Verlag, Berlin (1988).

[15] T. Hillen and H. G. Othmer. The diffusion limit of transport equations derived from velocity jump processes. SIAM J. Appl. Math. 61(3) (2000) 751-775.

[16] T. Hillen and K. J. Painter. A user's guide to PDE models for chemotaxis. J. Math. Biol. 58 (2009) 183-217.

[17] T. Hillen and A. Swan. The diffusion limit of transport equations in biology In: Mathematical Models and Methods for Living Systems, L. Preziosi et al (eds.) (2016) 73-129.

[18] R. Hoyle. Pattern formation: an introduction to methods. Cambridge University Press, Cambridge (2006).

[19] A. Kahana, G. Kenan, M. Feingold, M. Elbaum, and R. Granek. Active transport on disordered microtubule networks: the generalized random velocity model. Phys. Rev. E 78 (2008) 051912.

[20] C. Loverdo, O. Benichou, M. Moreau and R. Voituriez. Robustness of optimal intermittent search strategies in one, two, and three dimensions. Phys. Rev. E 80 (2009) 031146.

[21] H. G. Othmer and T. Hillen. The diffusion limit of transport equations II: chemotaxis equations. SIAM J. Appl. Math. 62(4) (2002) 1122-1250.

[22] S. Redner. Survival probability in a random velocity field. Phys. Rev. E 56 (1997) 4967-4972.

[23] H. Salman, A. Abu-Arish, S. Oliel, A. Loyter, J. Klafter, R. Granek and M. Elbaum. Nuclear localization signal peptides induce molecular delivery along microtubules. Biophys. J. 89 (2005) 2134-2145.

[24] P. J. Thomas and J. D. Cowan. Symmetry induced coupling of cortical feature maps. Phys. Rev. Lett. 92 (2004) 188101.

[25] D. Walgraef. Spatio-temporal pattern formation. Springer-Verlag, New York (1997).

[26] G. Zumofen, J. Klafte and A. Blumen. Enhanced diffusion in random velocity fields. Phys. Rev. A 42 (1990) 4601-4608.